Tectonophysics 710–711 (2017) 162–183

Contents lists available at ScienceDirect

Tectonophysics

journal homepage: www.elsevier.com/locate/tecto

From nappe stacking to extensional detachments at the contact between the Carpathians and Dinarides – The Jastrebac Mountains of Central Serbia

Dalibor Erak [a,b], Liviu Matenco [a], Marinko Toljić [b,*], Uroš Stojadinović [b], Paul A.M. Andriessen [c], Ernst Willingshofer [a], Mihai N. Ducea [d,e]

[a] Utrecht University, Faculty of Geosciences, Utrecht, The Netherlands
[b] University Belgrade, Faculty of Mining and Geology, Belgrade, Serbia
[c] VU University Amsterdam, Faculty of Earth and Life Sciences, Amsterdam, The Netherlands
[d] Department of Geosciences, University of Arizona, Tucson, AZ, USA
[e] University of Bucharest, Faculty of Geology and Geophysics, Bucharest, Romania

ARTICLE INFO

Article history:
Received 17 February 2016
Received in revised form 27 November 2016
Accepted 22 December 2016
Available online 29 December 2016

Keywords:
Kinematics
Thermochronology
Extensional detachments
Dinarides
Carpathians

ABSTRACT

Reactivation of inherited nappe contacts is a common process in orogenic areas affected by back-arc extension. The amount of back-arc extension is often variable along the orogenic strike, owing to the evolution of arcuated mountain chains during stages of rapid slab retreat. This evolution creates low rates of extension near rotation poles, where kinematics and interplay with the pre-existing orogenic structure are less understood. The amount of Miocene extension recorded by the Pannonian Basin of Central Europe decreases SE-wards along the inherited Cretaceous – Paleogene contact between the Dinarides and Carpathian Mountains. Our study combines kinematic data obtained from field and micro-structural observations assisted with fission track thermochronological analysis and U-Pb zircon dating to demonstrate a complex poly-phase evolution in the key area of the Jastrebac Mountains of Serbia. A first event of Late Cretaceous exhumation was followed by latest Cretaceous – Eocene thrusting and magmatism related to a continental collision that sutured the accretionary wedge containing contractional trench turbidites. The suture zone was subsequently reactivated and exhumed by a newly observed Miocene extensional detachment that lasted longer in the Jastrebac Mountains when compared with similar structures situated elsewhere in the same structural position. Such extensional zones situated near the pole of extensional-driven rotation favour late stage truncations and migration of extension in a hanging-wall direction, while directions of tectonic transport show significant differences in short distances across the strike of major structures.

1. Introduction

The formation of extensional back-arc basins is commonly associated with the rapid evolution of detachments re-activating inherited nappe contacts or rheological contrasts, as widely observed in Mediterranean or SE Asia orogens (Jolivet and Faccenna, 2000; Morley, 2012; Pubellier and Meresse, 2013; Vergés and Fernàndez, 2012). These extensional areas were created by slab retreat during the formation of highly arcuated mountain chains, where the amount of extension is variable along the strike of the orogen and is decreasing towards the poles of rapid rotation (e.g., Brun and Sokoutis, 2007, 2010; Faccenna et al., 2004; Wortel and Spakman, 2000; Zweigel et al., 1998). The evolution of extensional detachments reactivating inherited suture zones or nappe contacts is well studied in areas that display large amounts of extension (e.g., Brun and Faccenna, 2008; Hall et al., 2011). In contrast, the slow and prolonged deformation that affects areas situated near the pole of rotation in extensional back-arc basins is less known (e.g., Doglioni et al., 2007).

The evolution of the arcuated Carpathian mountain chain is controlled by the Miocene retreat of a slab attached to the European continent that has resulted in the formation of the large continental Pannonian back-arc basin (Fig. 1, e.g., Horváth et al., 2006; Horváth et al., 2015). The stretching in this extensional basin is laterally variable, but reaches ~220 km in a transect crossing the area of the Great Hungarian Plain (e.g., Balázs et al., 2016; Fodor et al., 1999; Tari et al., 1999; Tari et al., 1992). Recent studies near the southern Pannonian Basin margin have shown that the Miocene extension reactivated the latest Cretaceous – Paleogene suture zone of the Dinarides by forming a significant number of detachments distributed along its entire strike (Fig. 1, e.g., Ustaszewski et al., 2010; van Gelder et al., 2015). Owing to the rotational kinematics of the Carpathians and the interplay with the roll-back

* Corresponding author.
E-mail address: marinko.toljic@rgf.bg.ac.rs (M. Toljić).

http://dx.doi.org/10.1016/j.tecto.2016.12.022
0040-1951/

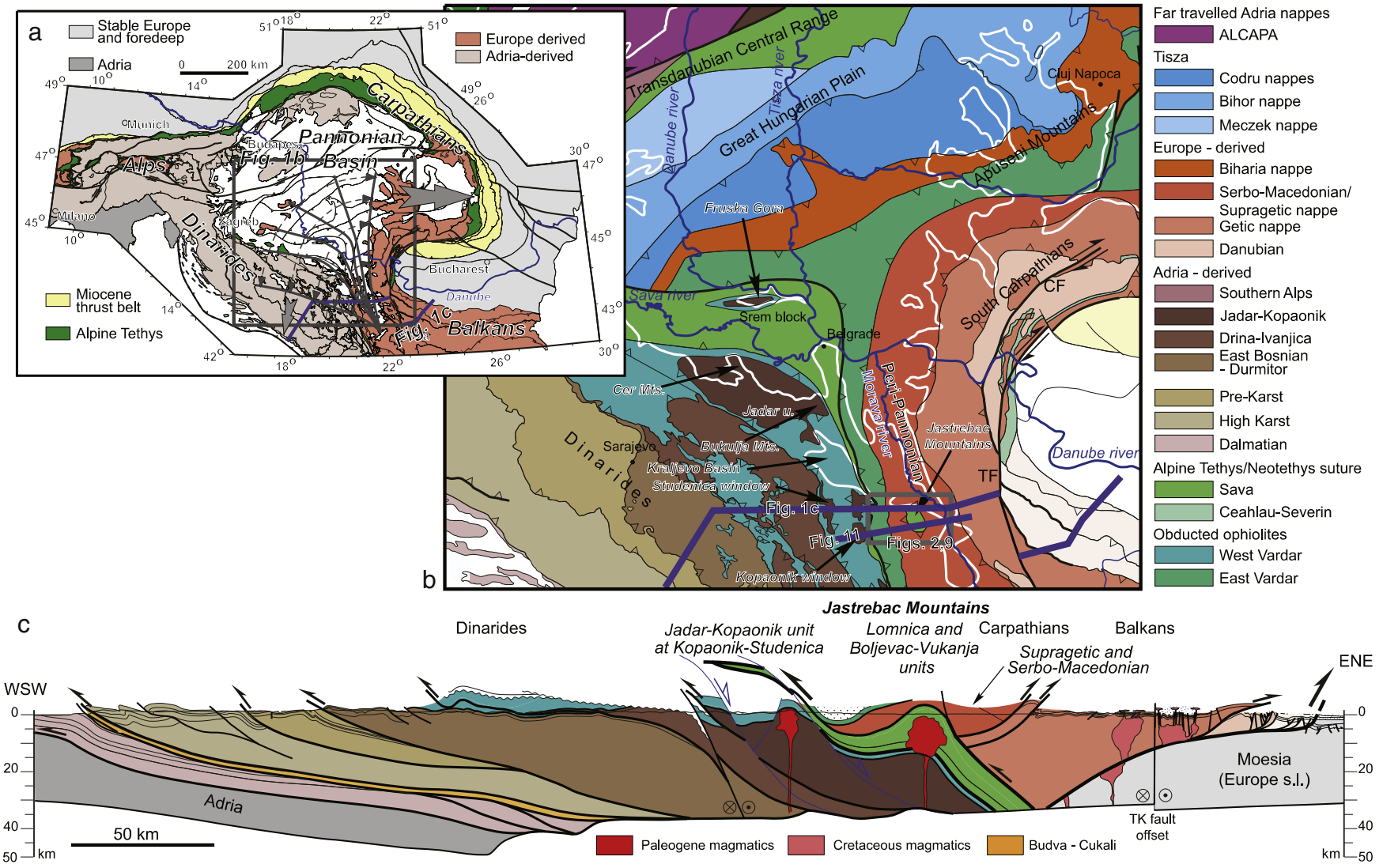

Fig. 1. a) Tectonic map of the Alps - Carpathians - Dinarides orogenic system with the extent of the Pannonian - Transylvanian back-arc basins (simplified from Schmid et al., 2008). The grey box indicates the location of the map in panel b, the thick blue line indicates the location of the cross section in panel c; The grey arcuated lines and arrows sketch the kinematics of extension in the Pannonian basin with a pole of rotation located in the southern part of the Morava corridor (adapted from Matenco and Radivojević, 2012). Grey arrows illustrate the directions of slab retreat that was larger in the Carpathians. b) Detailed tectonic map of the connecting area between the Dinarides and Carpathians Mountains (modified from Schmid et al., 2008). Note that the extent of the overlying Miocene-Quaternary basins is marked with white line, their structure and composition being ignored. The grey box is the location of the Jastrebac geological maps in Figs. 2 and 9. Thick blue lines are locations of the cross sections in Figs. 1c and 11. TF = Timok Fault; CF = Cerna Fault; c) Regional tectonic cross section with the structure of the Jastrebac Mountains in the overall context of the Dinarides and Carpathians (modified from Matenco and Radivojević, 2012). Location of the cross-section is displayed in panel b.

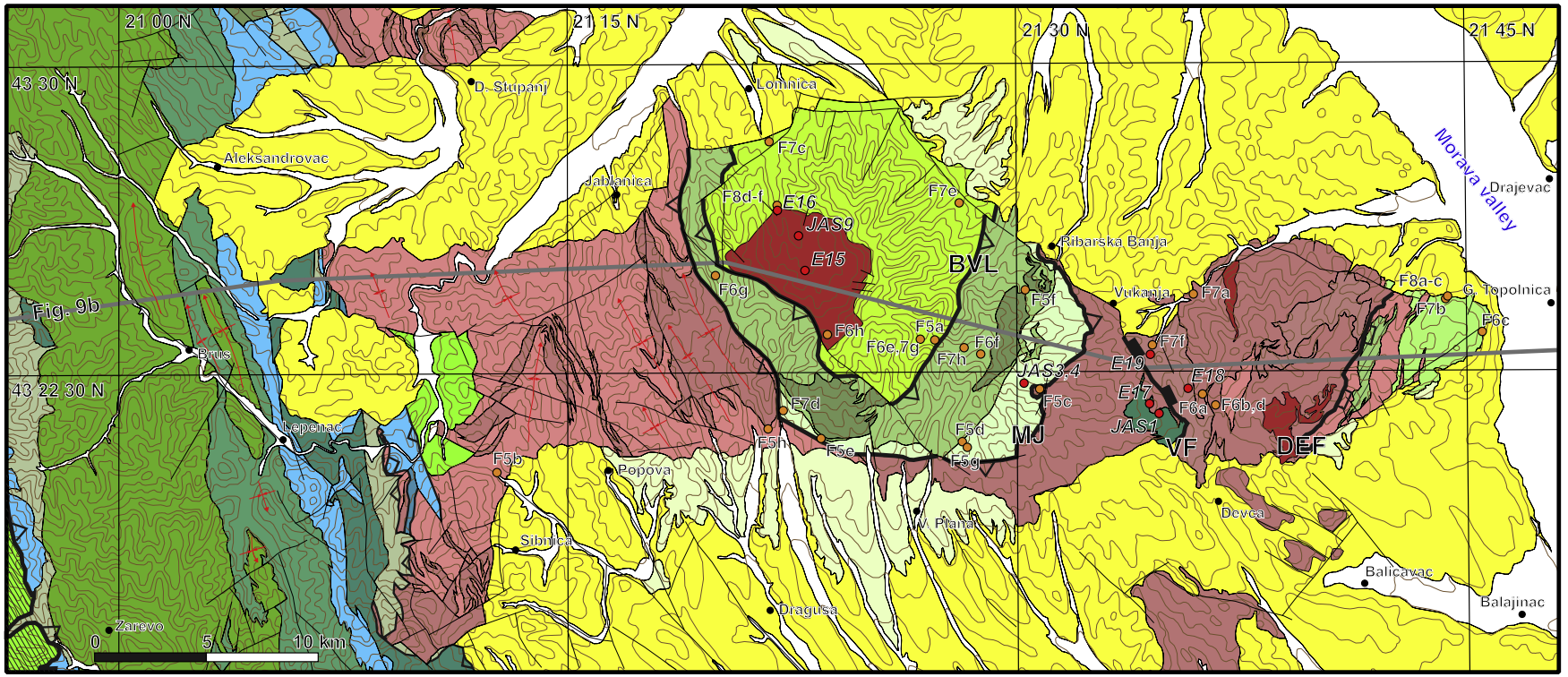

Fig. 2. Geological map of the Jastrebac Mountains area compiled and simplified from sheets of the 1:100.000 Geological Map of Yugoslavia and the results of the present study. The tectonic units nomenclature and the ages of tectonic unit contacts are taken from Marović et al. (2007) and Schmid et al. (2008), modified following the results of the present study. The thick grey line is the location of the cross-section in Fig. 11b. Red dots are the locations of zircons and apatite fission-track samples, the results being displayed in Fig. 10 and Tables 1 and 2. Yellow dots are the locations of field and micro-structural examples in Figs. 5–8. BVL - the contact separating the Boljevac-Vukanja and Lomnica sub-units of the Jastrebac unit; MJ - the contact separating the Morava and Jastrebac units; VF - Vukanja Fault; DEF - shear zone separating the Morava and Supragetic units. Note that this DEF zone is wider, shearing decreasing gradually W- and E-wards from the contact marked.

of the Dinaridic slab, the amounts of extension along detachments gradually decrease towards the SE roughly along the contact between the Carpathians and Dinarides (Fig. 1, e.g., Matenco and Radivojević, 2012; Stojadinović et al., 2013). In this SE area, an interesting structural situation is observed in the Jastrebac Mountains of Central Serbia, an isolated small inselberg of dominantly metamorphic rocks that is almost surrounded by the Miocene sediments of the Morava River corridor (Figs. 1 and 2). In this area, a tectonic window exposes a pluton intruding low-grade meta-turbidites and higher-grade meta-sediments and mafics, which are in tectonic contact with the surrounding high-grade metamorphic rocks of the Serbo-Macedonian Massif (Fig. 2). Existing studies have inferred that this tectonic contact formed during an initial nappe-stacking event and was later reactivated during an extension related to large-scale transcurrent motions along the orogenic strike (Grubić, 1999; Marović et al., 2007).

We aim to analyse the structure and exhumation of the Jastrebac Mountains to quantify the Cretaceous – Miocene evolution of the tectonic contact between the Dinarides and Carpathians. This quantification is important for understanding the mechanics of Miocene extension and associated deformation near the pole of the associated vertical axis rotation. We furthermore aim to understand the Cretaceous evolution and palaeogeographic affinity of tectonic units exposed in the Jastrebac Mountains by defining their position relative to the former Dinaridic suture zone. We have combined field kinematic observation with microstructural analysis, assisted by low-temperature thermochronology (zircon and apatite fission tracks) and high-temperature U-Pb zircon dating of the central pluton emplacement. The results are interpreted in the context of Dinarides evolution and general kinematics of extension.

2. The Jastrebac Mountains in the context of the Dinarides and Carpathians evolution

Situated at or near the contact between the Carpathians and Dinarides (Figs. 1c and 2), the Jastrebac Mountains contain the record of a complex tectonic evolution that was influenced by events taking place in both orogenic areas. Following the Middle - Late Triassic opening of a northern branch of the Neotethys (or Vardar) Ocean that in SE Europe separated Europe- from Adria- derived tectonic units, the SW to W facing Dinaridic orogen formed in response to the subsequent Late Jurassic – Paleogene closure of this oceanic domain (Fig. 1, e.g., Karamata, 2006; Robertson et al., 2009; Schmid et al., 2008). The Middle - Late Triassic opening was associated with basic to intermediate rifting magmatism and created a wide Adriatic passive continental margin. This margin recorded the gradual Middle Triassic – Lower Jurassic deepening of sedimentary facies observed in the internal Dinaridic units (e.g., Chiari et al., 2011; Dimitrijević, 1997; Djeric et al., 2007; Goričan et al., 2012; Monjoie et al., 2008; Pamic, 1984). The onset of subduction in the Neotethys Ocean was followed by Late Jurassic – earliest Cretaceous obduction over both the Adriatic and European margins. This has resulted in the emplacement of a ~180 km long sheet of ophiolites over the Adriatic margin, presently exposed in the internal Dinarides (Western Vardar Ophiolitic unit), and in the emplacement of ophiolites and island-arc volcanics over the European-derived Carpathian units (Eastern Vardar Ophiolitic unit) (Fig. 1, e.g., Dimitrijević, 1997; Robertson, 2006; Schmid et al., 2008). The subsequent Cretaceous – Paleogene shortening created a number of units thrust towards SW in the Dinarides, among which the most internal ones (East Bosnian - Durmitor, Drina - Ivanjica and Jadar - Kopaonik, Fig. 1) contain earlier obducted ophiolites in an upper structural position (Schmid et al., 2008). The distal part of the Adriatic margin was buried and locally metamorphosed by this nappe stacking. These metamorphosed rocks were subsequently exposed by tectonic exhumation in the footwall of a number of Miocene extensional detachments along the Dinarides strike (e.g., Schefer et al., 2010; Toljić et al., 2013; van Gelder et al., 2015 and references therein). A late Early Cretaceous tectonic event was followed by the onset of collision during latest Cretaceous times and the formation of the Sava Zone of the Dinarides. This suture zone contains dominantly Maastrichtian deep-water contractional trench turbidites (i.e. flysch deposits) (Fig. 1, e.g., Matenco and Radivojević, 2012; Pamić, 2002; Schmid et al., 2008; Ustaszewski et al., 2009). Widespread subduction-related magmatism started during the Late Cretaceous in the European back-arc domain (the Banatitic magmatism, ~92–67 Ma, e.g., Gallhofer et al., 2015 and references therein). The magmatism migrated gradually towards the internal Dinarides during the Paleogene, while becoming more crustal enriched, potassic or locally alkaline in a SW-ward direction, possibly due to the migration with time of the Dinaridic slab (Cvetković et al., 2000; Cvetković et al., 2013; Schefer et al., 2011). The shortening events were interrupted locally by a Late Cretaceous (Turonian - Campanian) episode of extension (Toljić, 2006; van Gelder et al., 2015).

Near the study area, the E- to NE-facing Carpathians orogen formed in response to the Cretaceous - Miocene closure of the Ceahlau-Severin Ocean that was part of the larger Alpine Tethys domain (Săndulescu, 1988; Schmid et al., 2008). The South Carpathians and their prolongation in Serbia closed already during successive stages of late Early (~100 Ma) and latest Cretaceous (~72–67 Ma) collision and nappe stacking. These events were followed by large-scale Paleogene - Early Miocene NE-ward translations and clockwise rotation accompanied by orogen parallel extension and the formation of large curved dextral strike-slip faults cumulating offsets in the order of 100 km (Timok and Cerna faults, Fig. 1b, Fügenschuh and Schmid, 2005; Iancu et al., 2005; Krautner and Krstic, 2002). This was subsequently followed by the Miocene - Quaternary collisional and post-collisional shortening of the East Carpathians accompanying their slab retreat (Ismail-Zadeh et al., 2012; Matenco et al., 2016). In the area adjacent to the Jastrebac Mountains (Fig. 1), the thrusting of the Supragetic over the Getic nappe took place during the late Early Cretaceous, as observed in the South Carpathians and their southward continuation in Serbia (Iancu et al., 2005; Krautner and Krstic, 2002). Further to the west, the Serbo-Macedonian "Massif" is part of the European-derived Dacia block (Figs. 1 and 2), and contains a medium- to high-grade metamorphic sequence locally overlain by proximal sediments of various Mesozoic ages (Dimitrijević, 1997). The age of amalgamation and metamorphism in the Serbo-Macedonian unit is considered Paleozoic due to its subsequent covering by Triassic non-metamorphic sediments (Karamata et al., 2003; Malešević et al., 1980; Meinhold et al., 2010; Ramovš et al., 1989). The contact between the Serbo-Macedonian unit and the Supragetic nappe is less understood due to its scarce exposures, but is generally thought to be affected by retrograde metamorphism during pre-Mesozoic times (Săndulescu, 1984) and, therefore, is considered to be Paleozoic or older in age. South of the study area, recent thermochronological studies have inferred that the peak metamorphic event in the Serbo-Macedonian unit is Variscan and that its magmatism had a long Paleozoic evolution (Antić et al., 2016a). This study interpreted a stage of exhumation during late Early to early Late Cretaceous times (~110–90 Ma), which was followed by other local exhumation events, such as the formation of neighbouring Eocene core-complexes (Antić et al., 2016b).

The internal Carpathians units and their contact with the Dinarides along the Sava suture were affected by the Miocene back-arc extension of the Pannonian Basin due to Carpathian slab roll-back (e.g., Horváth et al., 2015). A component of Dinarides slab roll-back has been invoked for the formation of the SE part of this basin, including the Morava corridor (Matenco and Radivojević, 2012). The inherited Sava Zone and other nappe contacts were reactivated by the formation of extensional detachments exhuming the previously buried distal Adriatic margin, a deformation that peaked at ~15–14 Ma (Schefer et al., 2011; Stojadinović et al., 2013; Ustaszewski et al., 2010). Although less documented in the Morava corridor (Fig. 1), the extension near the contact between the Carpathians and Dinarides started earlier (<29 Ma) and finished later (~8 Ma), when compared to other areas of the Pannonian Basin (Matenco and Radivojević, 2012; Toljić et al., 2013; Balázs et al., 2016).

2.1. The nappe structure and composition of the Jastrebac Mountains

The overall geometry of the Jastrebac Mountains is the one of a dome that is composed of two tectonic units, Morava and Jastrebac, the latter being sub-divided in two local sub-units, Boljevac - Vukanja and Lomnica (Fig. 2, Marović et al., 2007). All these units are separated by shear zones (MJ and BVL contacts in Fig. 2). The Morava unit is part of the much larger Serbo-Macedonian "Massif". At their easternmost corner, the Jastrebac Mountains expose a rare opportunity to study the contact between the Serbo-Macedonian and Supragetic units, which is otherwise commonly covered by Miocene sediments in Serbia (Fig. 2). In the west, the Morava unit is structurally overlain by the Eastern Vardar Ophiolitic unit and its overstepping Cretaceous, dominantly clastic sequence. The ophiolites and their overstepping sequence were thrust westwards over the uppermost Cretaceous syn-kinematic turbidites of the Sava suture zone (Figs. 1 and 2, see also Schmid et al., 2008).

2.1.1. The upper metamorphic unit

The Morava unit is composed of an association of high-grade metamorphic rocks, generally amphibolite-facies, which are locally affected by retrograde metamorphism in greenschist-facies conditions (Grubić, 1999; Marović et al., 2007). These rocks are composed of gneisses and micaschists of various compositions (garnet micaschists to dominant plagioclase-quartz) and migmatites that contain intercalations of quartzites, amphibolites, quartz-graphitic and graphitic schists, and marbles (Fig. 3). The overall sequence is locally intruded by granitic bodies of various sizes and compositions that are covered by Mesozoic strata. Morava unit along the western flank of the Jastrebac Mountains contains predominantly micaschists, while gneisses, migmatites and magmatic intrusions dominate their eastern part (Fig. 2). Along the eastern flank, fine gneisses with intercalations of amphibolites are observed from the contact with the Boljevac - Vukanja unit eastwards to the Vukanja Fault (between MJ and VF contacts, Fig. 2). From the Vukanja Fault eastwards, migmatites are gradually replaced eastwards by gneisses, micaschists and granitic intrusions. The ages of metamorphism and of the protolith in this high-grade sequence are unknown in the Jastrebac Mountains, but are inferred to be Paleozoic by correlation with the larger Serbo-Macedonian unit (e.g., Grubić, 1999). The Morava unit in the Jastrebac Mountains has been affected by a complex poly-phase deformation history that includes micro- to cm-scale superposed folding events, subsequently affected by larger scale cylindrical folds oriented NNW-SSE (Grubić, 1999; Marović et al., 2007). These studies have interpreted the Vukanja Fault (Fig. 2) as a sinistral strike-slip shear zone associated with the transtensional exhumation of the mountains. At the eastern termination of the Jastrebac Mountains, the Supragetic unit crops out in structural contact with the gneisses and

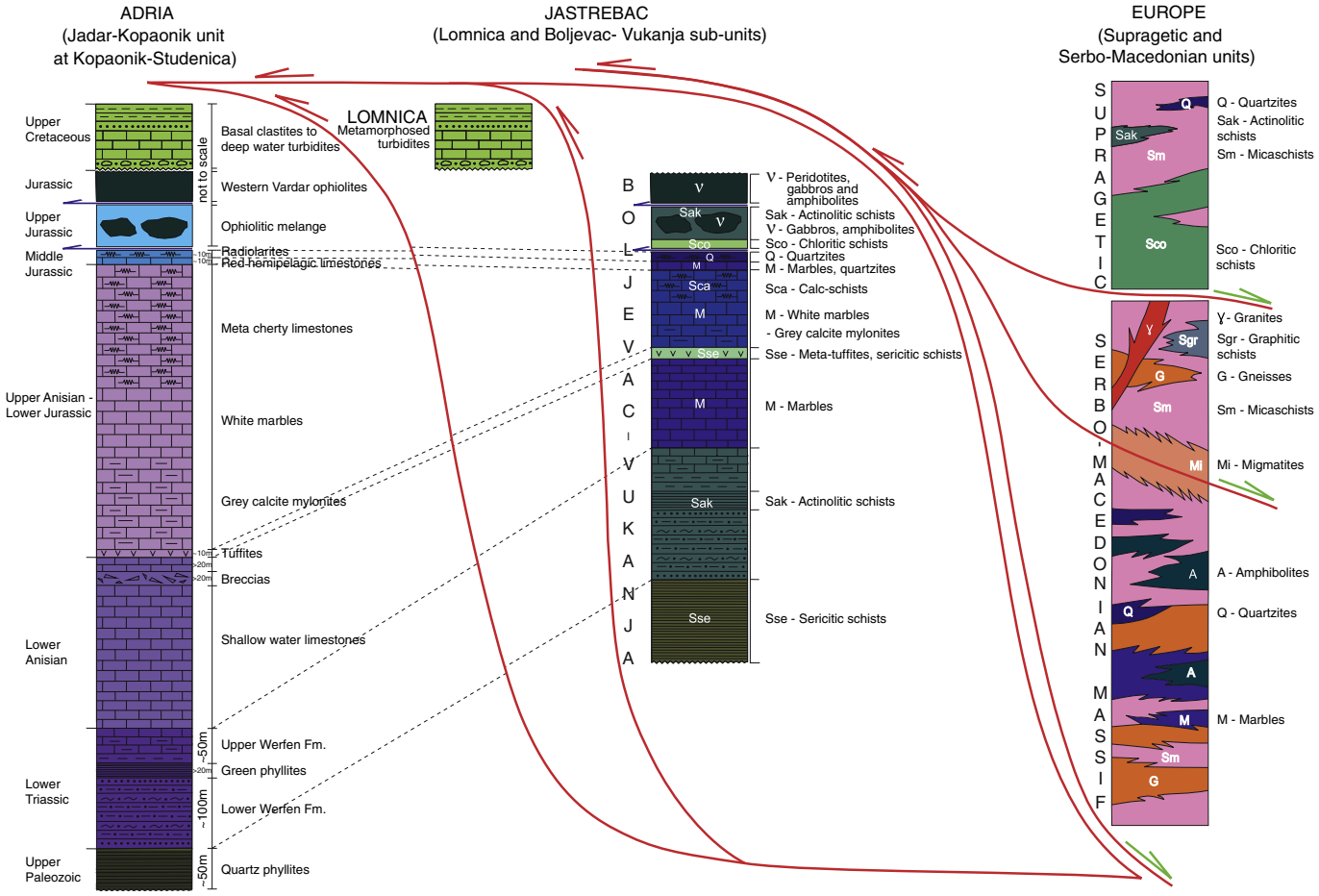

Fig. 3. Tectonic and lithostratigraphic columns with correlation between the metamorphic units of the Jadar-Kopaonik units (left) observed in the footwall of the Studenica and Kopaonik detachments (Schefer et al., 2011; Schefer et al., 2010) with the metamorphic rocks of the Jastrebac unit (centre) and the ones of the Morava unit (right) in the area of the Jastrebac Mountains (modified from Marović et al., 2007). The overall correlation follows the results of the present study by using the tectonic scheme of Schmid et al. (2008). Similar lithostratigraphic and facial correlations are also available in other areas of the Dinarides (e.g., Toljić et al., 2013; van Gelder et al., 2015). Blue fault half-arrow signatures illustrate the Late Jurassic - earliest Cretaceous obduction, while the subsequent contraction and extension are marked with red and green half-arrows, respectively.

micaschists of the Morava unit (Fig. 2, Krautner and Krstic, 2002). The Supragetic unit contains lower degree metamorphic rocks, mainly chloritic schists and micaschists, with intercalations of quartzites, actinolitic schists, amphibolites and amphibolite gneisses (Fig. 3).

2.1.2. The lower metamorphic unit

Located structurally in a lower position when compared to the Morava unit, the Jastrebac unit builds the centre of the mountains and is separated in a lower Lomnica and a higher Boljevac-Vukanja sub-unit by a tectonic contact (BVL in Fig. 2, Marović et al., 2007). The lower Lomnica sub-unit contains a low-degree, sub-greenschist to lower greenschist-facies meta-sedimentary rock sequence that formed from a dominantly coarse-grained turbiditic protolith with significant lateral variations (Pantić et al., 1969; Rakić et al., 1976). This sequence contains rare fossil remnants of Upper Cretaceous-Paleogene in age (Marović et al., 2007; Rakić et al., 1976). In its centre, the Lomnica sub-unit is intruded by the Ravnište pluton (Fig. 2) that is composed dominantly of a granodiorite associated with outcrop-scale intrusions, and felsic dykes and sills cross-cutting the neighbouring meta-sediments, which are well developed east and southeast of the main intrusion. These sediments are also affected by metasomatic mineral growth and exhibit an increase in metamorphic grade in the contact zone. A final phase of igneous activity is observed by the occurrence of aplitic and quartz veins. Previous whole-rock Rb-Sr thermochronological dating implied a 37.3 ± 5 Ma age of the pluton (Červenjak et al., 1963; Grubić, 1999). The meta-sedimentary unit is significantly deformed with at least two phases of folding associated with the formation of axial plane cleavages and folds with a symmetrical orientation observed in the immediate vicinity of and around the dome (Grubić, 1999; Marović et al., 2007).

The structurally higher Boljevac-Vukanja sub-unit contains a large variety of rocks generally metamorphosed in a higher greenschist-facies when compared with the Lomnica sub-unit (Figs. 2 and 3). The main mass is composed of epidote-, actinolite-, sericite- and chlorite-bearing schists, quartzites, phyllites, marbles and calcschists that contain large bodies of amphibolites and peridotites (Fig. 2). The amphibolites often contain gabbroic textures. The presence of a more sericitic - quartzitic zone at the margin of the dome and a more actinolitic one in the centre is generally regarded to reflect a further unit separation, although the transition between them is gradational (Rakić et al., 1976; Krstić et al., 1980). The meta-limestones contain deformed Mesozoic or early Tertiary fauna (Krstić et al., 1980). The protolith age and tectonic affinity of rocks exposed in the Boljevac-Vukanja sub-unit is still a matter of debate. The protolith age of these rocks was interpreted Paleozoic and younger (Rakić et al., 1976), or partly Late Cretaceous - Paleogene (Marović et al., 2007). These rocks were interpreted to be derived from the Carpatho-Balkanides (Krstić et al., 1980), or more specifically from the Supragetic nappe of the Carpathians nappe stack (Grubić, 1999).

2.1.3. The overlying ophiolites and sedimentary cover

The obducted ophiolites of the Vardar zone (sensu Dimitrijević, 1997) or the Eastern Vardar Ophiolitic unit (sensu Schmid et al., 2008) structurally overlie the Morava unit along the western termination of the Jastrebac Mountains (Figs. 2 and 3). The ophiolitic melange is exposed in narrow elongated zones beneath the ophiolites and is made up of blocks of dunites and serpentinised harzburgites (Rakić et al., 1972) in a dismembered melange containing dolerites, pillow basalts, pre-Tithonian radiolarites and deep-water shales (Rakić et al., 1976) together with more shallow-water detritus such as carbonatic sandstones and conglomerates that were deposited during obduction (Rakić et al., 1972). In a structurally higher position, the ophiolites are composed of large elongated zone of dolerites, serpentinites and peridotites (Fig. 2). An overstepping sequence, which starts with Tithonian shallow-water limestones and continues with transgressive Berriasian-Cenomanian clastic-carbonatic sediments (the "paraflysch" of Karamata, 2006; Dimitrijević, 1997; Dimitrijevic and Dimitrijevic, 1987), overlies the entire ophiolitic unit along the western flank of the Jastrebac Mountains. Upper Cretaceous conglomerates, shallow-water deposits and turbidites were deposited transgressively over the Morava basement along the western flank of the dome (Fig. 2).

In the westernmost part of the study area, the ophiolitic unit and its overstepping sequence are thrust over the typical uppermost Cretaceous sediments of the Sava zone (Figs. 2 and 3). These sediments border to the east the structure of the Kopaonik Mountains (Fig. 1b) and recorded pelagic and turbiditic sedimentation with periodic influxes of significant ophiolitic detritus that recorded the closure of the Neotethys and the formation of the suture zone, which was significantly reactivated during the later Miocene extensional event (Schefer, 2010).

Neogene sediments surround and their upper part unconformably overlie the tectonic units of the Jastrebac Mountains (Fig. 2, see also Marović et al., 2007). These Lower - Middle Miocene transgressive sediments show a continental alluvial and conglomeratic facies passing gradually to a shallow-water lacustrine and eventually to marine deposition. Following an unconformity near the limit between the Middle and Upper Miocene, the overlying sedimentation is regressive and changes gradually back to lacustrine and continental Late Miocene - Pliocene sedimentation.

3. Field and micro-structural observations.

Field kinematic observations included measurements of foliations, folds, ductile shear zones and associated stretching lineations, brittle faults and other cataclastic structures, combined with observations of post-kinematic tilting and rotations. Brittle slickensides and Riedel shears together with more ductile kinematic indicators in shear zones, such as shear bands or sigma clasts were used to derive the tectonic transport directions. These observations were generally grouped in deformation events (Fig. 4) and presented as examples of representative outcrop structures (Figs. 5–7). Superposition criteria, such as the evolution of the metamorphic facies, stratigraphic constraints, overprinting mineral associations, truncations, tilting, syn-kinematic sedimentary wedges or post-kinematic deposition were used to derive the relative or absolute timing of deformation. The microstructural observations were used to define the metamorphic facies associations and to study the kinematics of deformation (Fig. 8).

The oldest deformational structures recorded in the Jastrebac Mountains are observed in the amphibolite-facies rocks of the Morava unit. These structures are small-scale (cm-scale to microstructures) crenulations and isoclinal folds in meta-sediments and, in few places, in meta-magmatic rocks (gneisses, migmatites, amphibolites). These small-scale structures are not observed in the Jurassic-Cretaceous cover overlying the Morava basement and are affected in all observed situations by the subsequent deformations described below. Therefore, these structures must be older and most likely formed during the Paleozoic events that affected the larger Serbo-Macedonian unit. This interpretation is comparable with similar structures and age relationships observed outside the study area (for further details see Kydonakis et al., 2014; Antić et al., 2016a, 2016b). This deformation event is outside the scope of our study and will not be discussed further (i.e., pre-dates our D1-D5 sequence of tectonic events discussed below).

The main metamorphic foliation in all units of the Jastrebac Mountains is gently dipping roughly W- or E-wards away from a centre located in the middle of the central Lomnica unit. This shows a dome type of structure (Fig. 4a, see also Marović et al., 2007). This is affected by multi-stage folding combined with multiple stages of brittle and ductile shearing (Fig. 4), which testifies a poly-phase post-Paleozoic deformation history of the Jastrebac Mountains. We further describe this deformation history by grouping structures in phases of deformation based on their superposition criteria and analyse their variability in different tectonic units. Such grouping may include structures formed in different temperature conditions that are exposed in outcrops by burial and/or

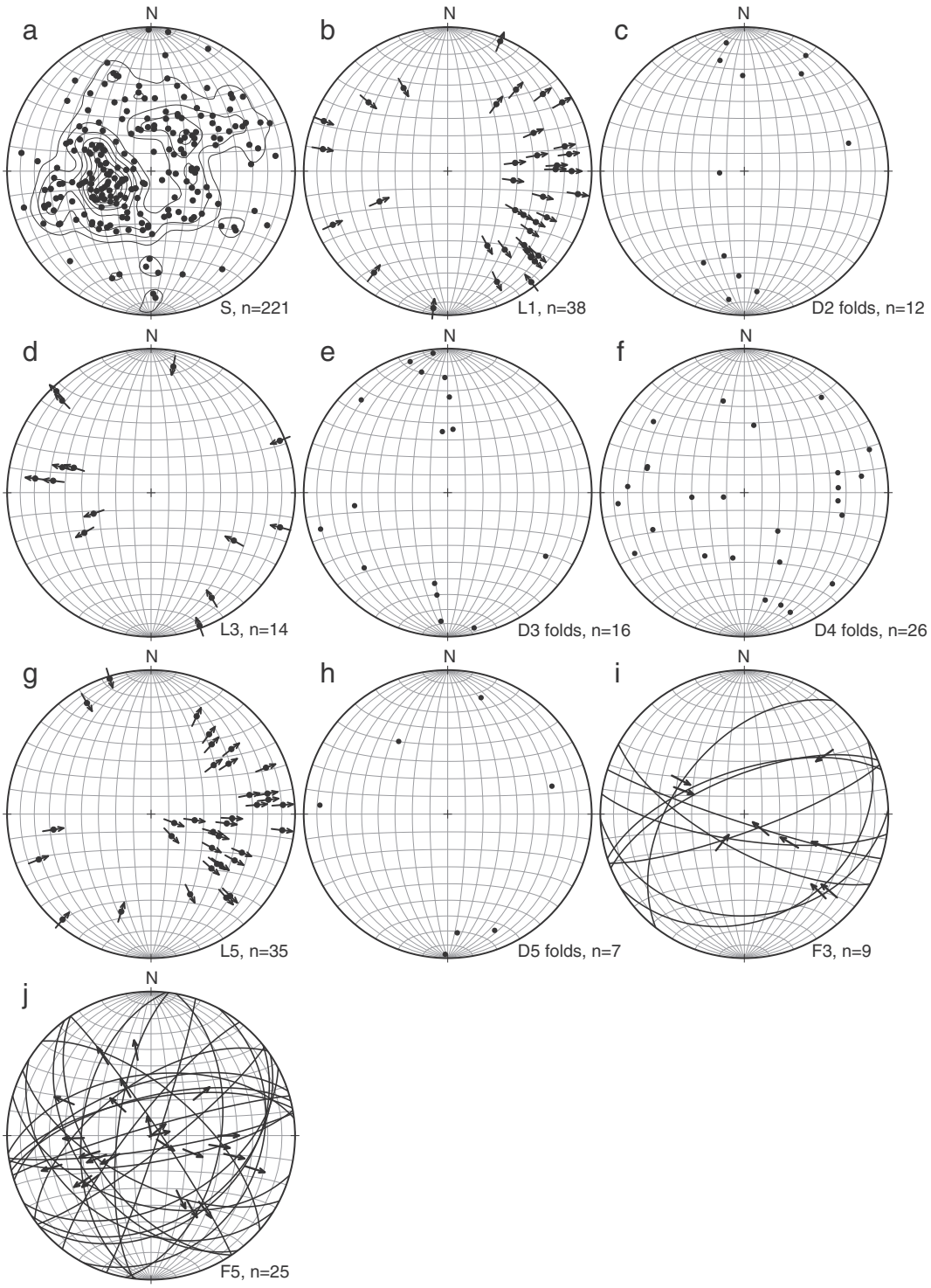

Fig. 4. Structural data measured in the area of the Jastrebac Mountains. All plots are Schmidt net projections, lower hemisphere. a) Stereoplots and density contours of the poles of the main foliation in the metamorphic rocks of the Morava and Jastrebac units. Note that the foliation is generally low angle dipping and generally follows the N-S oriented antiformal structure of the Jastrebac Mountains; b) Stretching lineations with the sense of shear for the oldest (D1) stretching event, derived from outcrop measurements and microstructural observations (blue arrows in Fig. 9). Note that these stretching lineations were found exclusively in the Morava and Supragetic units located east of the Vukanja Fault. c) Axes (hinges) of isoclinal folds associated with the second (D2) deformation event; d) Stretching lineations with the sense of shear for the third (D3) top-W stretching event, derived from outcrop measurements and microstructural observations (green arrows in Fig. 9); e) Axes (hinges) of asymmetric folds associated with the third (D3) deformation event; f) Axes (hinges) of upright folds associated with the fourth (D4) deformation event; g) Stretching lineations with the sense of shear for the fifth (D5) top-E stretching event, derived from outcrop measurements and microstructural observations (orange arrows in Fig. 9); h) Axes (hinges) of folds with sub-horizontal axial planes associated with the fifth (D5) deformation event; i) Brittle reverse to transpressional faults (plotted as fault planes with direction of motion and sense of shear) observed in the field; j) Normal faults (plotted as fault planes with direction of motion and sense of shear) observed in the field.

exhumation either during one tectonic event or by subsequent vertical movements at tectonic contacts. We note that kinematic observations are quantitatively relevant given the relatively small-size of the Jastrebac Mountains with reduced exposures in outcrops, which is otherwise similar with many other studies in such inselbergs of the Pannonian Basin (e.g., Toljić et al., 2013).

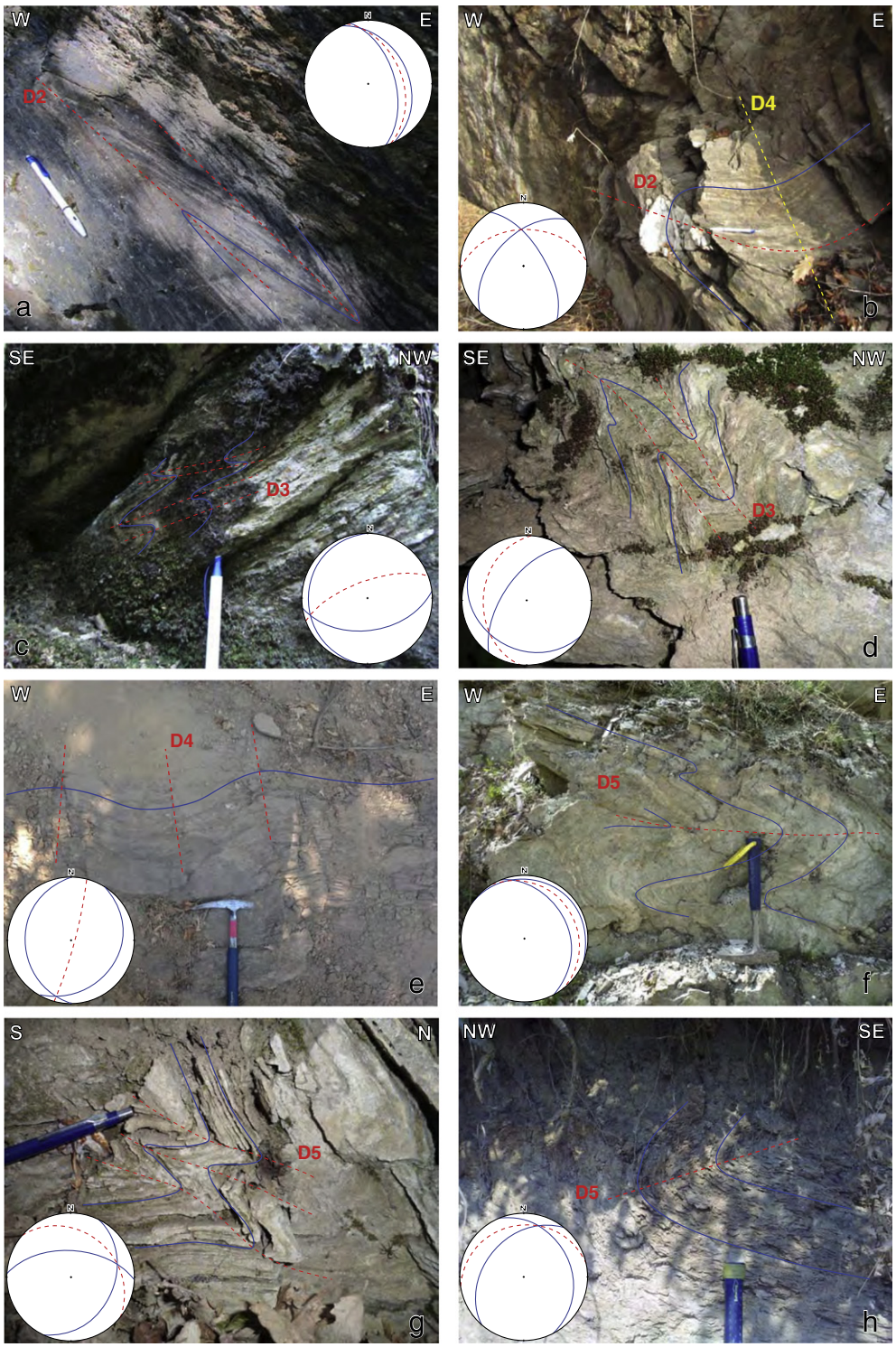

Fig. 5. Field examples of the structures described in the present study. Location of outcrops is displayed in Fig. 2. Structural elements are projected in stereoplots with the same colour as used in photos. Blue - foliation; red and yellow - axial planes. a) Isoclinal folds (D2) observed in the uppermost Cretaceous meta-turbidites of the Lomnica sub-unit along the E flank of the dome; b) Isoclinal fold (D2) refolded by a symmetric fold (D4) in the micaschist of the Morava units along the WSW flank of the dome; c) Asymmetric folds (D3) observed in the gneisses of the Morava unit along the E flank of the dome; d) Asymmetric folds (D3) in sericitic schists of the Boljevac - Vukanja sub-unit along the SE flank the dome; e) Upright folds (D4) in the greenschists of the Boljevac - Vukanja sub-unit along the S flank of dome; f) Folds with sub-horizontal axial planes (D5) observed in the actinolitic schists of the Boljevac - Vukanja sub-unit along the E flank of the dome; g) Folds with sub-horizontal axial planes (D5) in sericitic schists of the Boljevac - Vukanja sub-unit along the SE flank the dome; h) D5 fold with sub-horizontal axial plane in micaschists of the Morava unit along the SW flank of the dome.

In summary, the overall deformation history observed in the study area includes a D1 ~top-E stretching event, followed by a contractional event composed of three phases (D2 isoclinal folding, D3 asymmetric folding and top-W stretching and D4 open folding with sub-vertical axial planes), ultimately overprinted by an D5 event of top-E stretching, brittle normal faulting and formation of folds with sub-horizontal axial planes (Figs. 4–8).

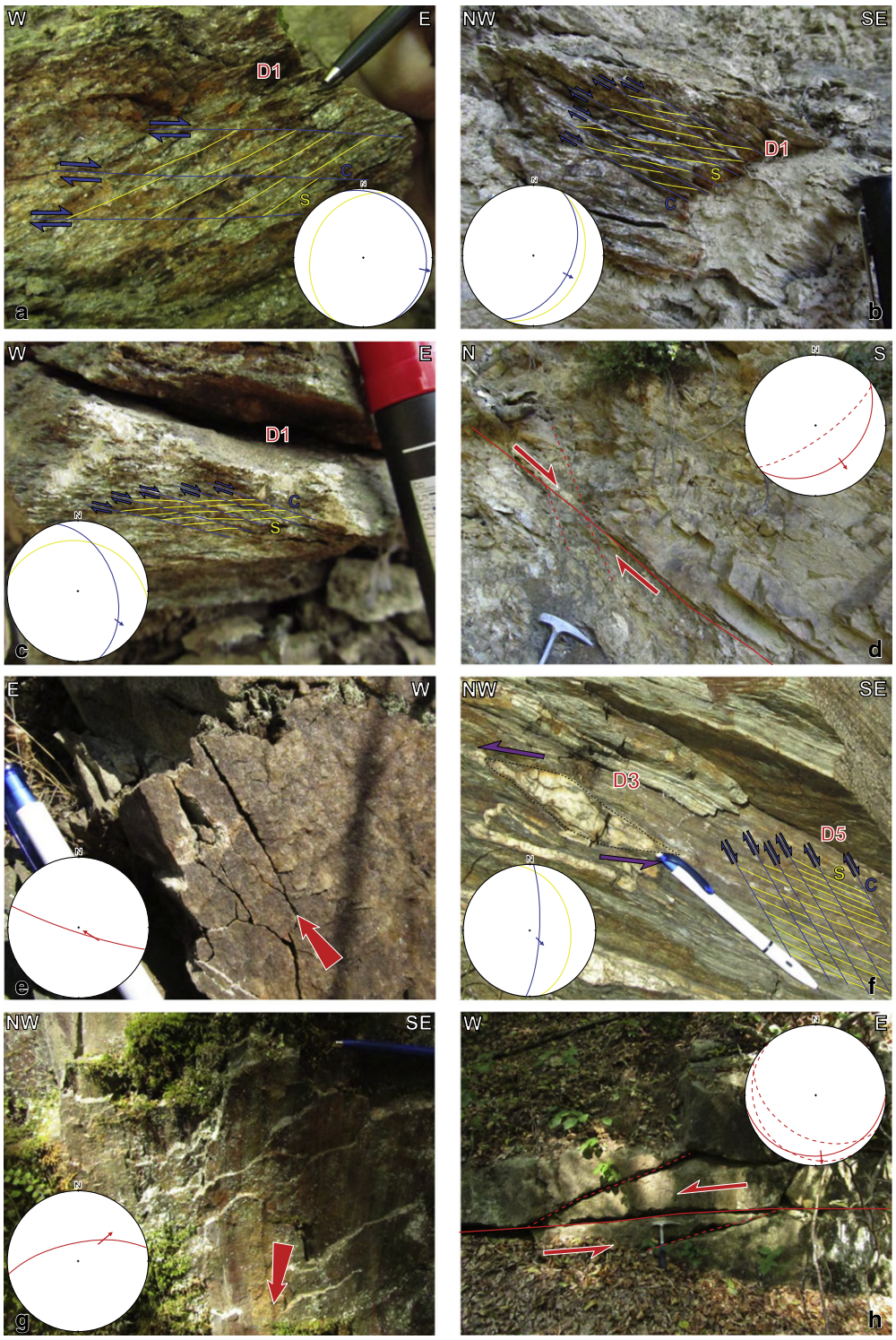

Fig. 6. Field kinematic examples of structures and shears with kinematic indicators observed in the present study. Location of outcrops is displayed in Fig. 2. Structural elements are projected in stereoplots with the same colour indicated in photos. Yellow- foliation, blue - shears, red - faults and Riedels, dashed red - projected Riedel. a) Shear-bands indicating top-E sense of shear (D1) in the migmatites of the Morava unit located east of the Vukanja Fault; b) Shear-bands indicating top-SE sense of shear (D1) in gneisses and micaschists of the Morava unit located E of the Vukanja Fault; c) Shear-bands indicating top-E sense of shear (D1) in the chloritic schists of the Supragetic nappe located at the eastern termination of the dome; d) normal fault with Riedel shears indicating top-SE sense of shear (D1) in the gneisses of the Morava unit east of the Vukanja Fault; e) Hanging-wall of a thrust fault (D3) indicating top-NW sense of shear in the uppermost Cretaceous meta-sandstones of the Lomnica sub-unit along the E flank of Jastrebac dome.; f) Superposition relationship between top-NW (D3) shearing (see sigma-clast on the left) and subsequent (D5) shear bands indicating top-SE sense of shear in the actinolitic schist of Jastrebac unit on the eastern flank of the dome; g) Hanging-wall of a normal fault and slickensides with top-NE sense of shear (D5) in the actinolitic schists of the Boljevac - Vukanja sub-unit along the western flank of the dome; h) The sub-horizontal part of a listric normal fault with Riedel shears indicating top-S sense of shear (D5) in the Jastrebac granodiorite along the W flank of the dome.

Fig. 7. Field kinematic examples of structures and shears with kinematic indicators observed in the present study. Location of outcrops is displayed in Fig. 2. Red arrows - sense of shear. a) Sigma-clast indicating top-SE sense of shear (D1) in the gneisses of the Morava unit located E of the Vukanja Fault; b) Sigma-clast indicating top-E sense of shear (D1) in the chloritic schists of the Supragetic unit at the eastern termination of the dome; c) Sigma-clast indicating top-NW sense of shear (D3) in uppermost Cretaceous meta-sandstones of the Lomnica sub-unit along the W flank of Jastrebac dome; d) Sigma-clast indicating top-NW sense of shear associated (D3) in sericitic schists of the Lomnica sub-unit along the W flank of Jastrebac dome; e) Sigma-clast indicating top-NW sense of shear (D3) in uppermost Cretaceous meta-sandstones of the Lomnica sub-unit along the E flank of the dome; f) Sigma-clast indicating top-NNE sense of shear (D5) in the migmatites of the Morava unit located E of the Vukanja Fault; g) Sigma-clast indicating top-SE sense of shear (D5) in the uppermost Cretaceous meta-sandstones to meta-pelites of the Lomnica sub-unit along the E flank of the dome; h) Sigma-clast indicating top-NNE sense of shear (D5) in the actinolitic schists of the Boljevac - Vukanja sub-unit along the E flank of the dome.

3.1. Shearing with ~top-E sense of transport (D1)

The first deformation event (D1) is well-observed in the Morava and Supragetic units located east of the Vukanja Fault (Fig. 2). This deformation is more difficult to discriminate west of the Vukanja Fault, due to strong overprint by subsequent shearing and metamorphism. D1 is characterized by shearing with a dominant top-E sense of tectonic transport, which consistently cuts through the older small-

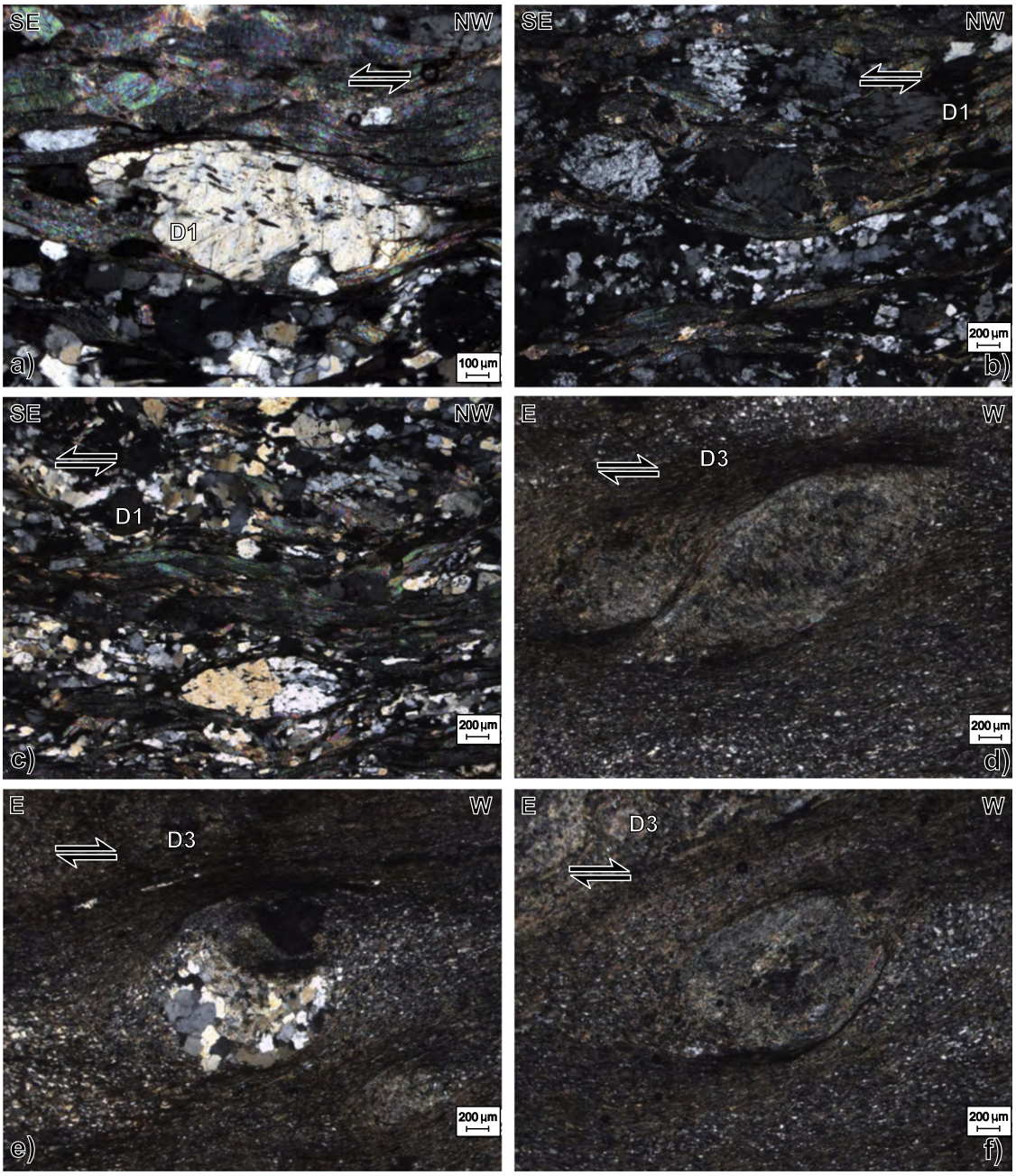

Fig. 8. Examples of micro-structures with sense of shear indicators observed in the present study. Location of outcrops is displayed in Fig. 2. Black arrows - sense of shear. a–c) Sigma-clast and mica-fishes showing top-SE sense of shear (D1) in the schists located E of the Vukanja Fault; d–f) Sigma-clasts showing a top-W sense of shear (D3) in the Upper Cretaceous meta-sandstones of the Lomnica sub-unit along the western flank of the dome.

scale crenulations and isoclinal folds of interpreted Paleozoic age in all observed situations. The shearing locally diverges more to NE, NNE, SE and SSE (Fig. 4b, blue arrows in Fig. 9a), because of partial re-orientation by subsequent deformation, either folding, faulting or other shearing events. In outcrops, D1 deformation is observed mainly by structures indicating shearing of the high-degree metamorphics of the Morava unit. The migmatites, micaschists and gneisses are affected by stretching, which is often observed in mm-dm scale shear bands (Fig. 6a,b). These indicate top-E sense of transport wherever these rocks are less affected by subsequent deformation. Porphyroclasts such as feldspars and garnet form often asymmetric shear sense indicators such as sigma or delta clasts (Fig. 7a). Similar features are also observed in the Supragetic unit located at the eastern termination of the dome (Figs. 6c, 7b), where shearing was associated with lower greenschist-facies metamorphism. Therefore, D1 shearing affected both the Morava and Supragetic units in a wide zone east of the Vukanja Fault (Fig. 9a). In outcrops, this ductile shearing is truncated by or changes laterally to more cataclastic to brittle features, such as normal faults that have similar top-E to top-SE kinematics (e.g., Fig. 6d). These observations suggest that deformation was associated with exhumation to shallower structural levels, although observed structures are not fully diagnostic. This is important because a clear separation from the cataclastic to brittle features of the younger extensional event (D5) is rather difficult. Therefore, these D1 normal faults were not separated in our plots from the subsequent D5 ones (Fig. 4j).

In thin sections, the mylonitic fabric (Fig. 8a–c) is associated with a foliation and many kinematic indicators such as sigma clasts and mica fishes. Alternating bands of mylonites and proto-mylonites show that deformation has the tendency to focus on narrow shear zones. Coaxial flattening is locally observed by elongation of feldspars and quartz

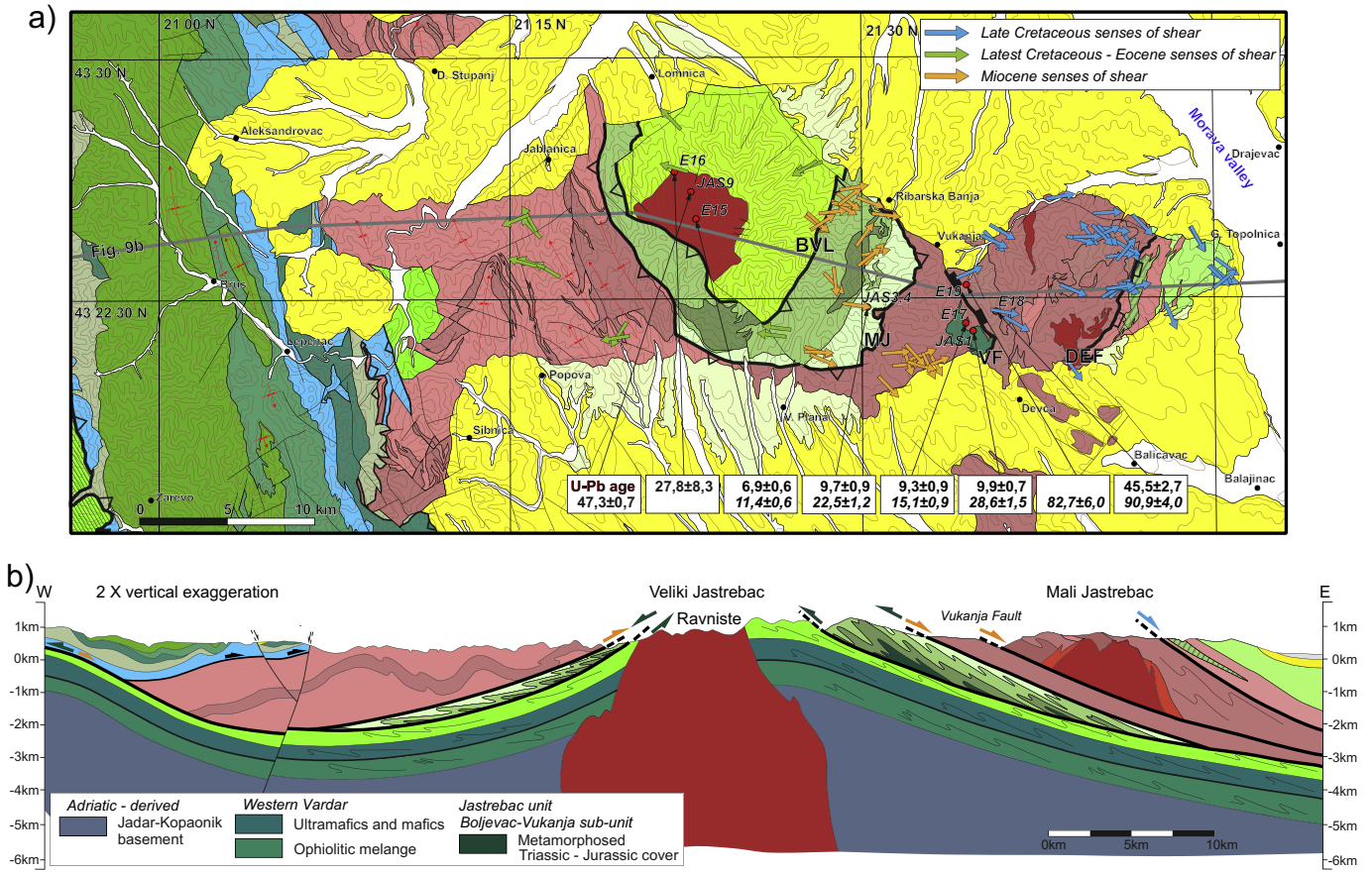

Fig. 9. Kinematic and thermochronological results of the present study. The colours in the map and cross sections follow the legend available in Fig. 2, except for units exposed only in the subsurface presented in the cross-section. a) Geological map of the Jastrebac Mountains area (same conventions as in Fig. 2) with the kinematic senses of ductile shear and the thermochronological ages determined by the present study. Thick grey line is the location of the geological cross-section in panel b. The age marked with orange affected by the metasomatism of the pluton and not used in the interpretation (see the text for further details). BVL - the contact separating the Boljevac-Vukanja and Lomnica sub-units of the Jastrebac unit; MJ - the contact separating the Morava and Jastrebac units; VF - Vukanja Fault; DEF - the shear zone separating the Morava and Supragetic units. Note that the DEF is a wide zone of distributed deformation which decreases gradually W- and E-wards from the marked contact. Blue arrows - D1, green arrows - D3, orange arrows - D5. b) Geological cross-section crossing the Jastrebac dome and adjacent areas. Note that the depth interpretation is estimative and is derived from surface projection along and across the strike of structures. Note also the 2× vertical exaggeration. Location of the cross-section is displayed in panel a. Half-arrows are senses of shear at contacts between units, the colour significance is the same as in panel a.

aggregates, and by subordinated coeval shearing in opposite direction. Microstructures show a strong tendency of focussing deformation on inherited foliations. The shearing in the overall high-grade metamorphic assemblage of the Morava unit implies that deformation was associated with lower-grade metamorphic conditions, as indicated by grain-size reduction and transformation into low-grade minerals such as chlorite or sericite. The observed metamorphic assemblage indicates temperatures around 400 °C. In our samples taken from the Morava unit, this assemblage postdates an earlier phase of peak metamorphism in amphibolite-facies conditions, which is presumably Paleozoic.

3.2. Contractional deformation (D2-D4)

Contractional structures were observed to postdate the D1 deformation and pre-date the younger extensional event. In more detail, superposition criteria observed in the field suggest a further separation in successive contractional phases. However, some of these phases are documented by a relatively low amount of kinematic observations (Fig. 4). These observations are relevant at the relatively small scale of the Jastrebac Mountains, but do not allow a further separation of tectonic events. Therefore, we have grouped these successive contractional phases into one tectonic event. The structures associated with this deformation are better expressed west of the Vukanja Fault (Fig. 2).

The first phase of contraction (D2) is associated with the formation of a foliation (S2) associated with tight isoclinal folding (F2). In the Jastrebac and Lomnica units this foliation formed by the transposition of an initial bedding and was also associated with isoclinal folding. In other words, the transposition of sedimentary bedding together with the axial plane cleavage of isoclinal folds form together a composite foliation. In the Morava and Supragetic units the S2 is an axial plane foliation of F2 isoclinal folds, which overprints older smaller-scale crenulations and isoclinal folds of interpreted Paleozoic age. D1 shears are re-folded by D2 isoclinal folds east of the Vukanja Fault, whereas such superposition was more difficult to observe westwards due to the subsequent overprint by ductile shearing and metamorphism. The S2 foliation builds up the low-angle dipping geometry on both flanks of the dome (Fig. 4a). The axes of outcrop-scale isoclinal F2 folds (Fig. 5a) are oriented predominately in the N-S to NNE-SSW direction (Fig. 4c). Decimetre- to metre- scale D2 isoclinal folds are particularly well visible in the Morava unit between the contact with the Jastrebac unit and the Vukanja Fault (between MJ and VF, Fig. 2), locally re-folded by subsequent deformational events (e.g., Fig. 5b). F2 axial planes dip gently E- or W-wards with axes plunging slightly N- or S-wards (Fig. 4c).

The second phase of contraction (D3) is observed by asymmetric folds, top-W shearing and reverse faults (Figs. 4d,e and 9a), which occur both in the low-grade metamorphic core and in the high grade

metamorphic flanks. Like the isoclinal folding, the asymmetric folds (D3) plunge gently NW- or SW-wards, albeit with significant spread (Fig. 4e). In outcrops, the asymmetric folds are often decimetre- to metre- in size (Fig. 5c,d). These folds are better observed in densely foliated lithologies such as micaschists, calcschists or other schistose rocks. Evidence of shearing and kinematic indicators (Fig. 4d, green arrows in Fig. 9a) are obvious in the meta-sediments of the Lomnica sub-unit (Fig. 7c–e), where sheared feldspars or quartz intercalations displays often sigma clast fabrics. The degree of metamorphism during this shearing decreases more to the west in the Morava unit, where brittle S-C fabrics were associated with this deformation phase. In thin sections, the mylonitic fabric is similarly associated with shear bands and sigma clasts developed during the weak metamorphic growth in the low greenschist-facies meta-sediments of the Lomnica sub-unit (Fig. 8d–f). D3 deformation phase also created reverse brittle faults, which are observed in all units of the Jastrebac Mountains (e.g., Fig. 6e). These are reverse faults that indicate NW-SE contraction, sometimes tilted or rotated by subsequent deformation (Fig. 4i). We justify grouping of these brittle and ductile structures into a single deformation phase by coeval burial, which brought rocks west of the Vukanja Fault from shallow brittle to metamorphic conditions during the D3 phase of contraction.

The third phase of contraction (D4) formed open and upright symmetrical folds (Fig. 4f). In outcrops, these folds are generally metre-scale and re-fold earlier contractional structures (Fig. 5b,e) and were observed in all units of the Jastrebac Mountains. The hinges and axial planes of these folds do not display a preferential direction (Fig. 4f) and we grouped these folds by following the character and superposition of deformation. In more detail, the plunge direction of fold axes follows the overall dome structure of the Jastrebac Mountains and the centrally emplaced pluton, implying a direct genetic relationship.

3.3. Extensional deformations (D5)

The last significant deformation event (D5) comprises both brittle and ductile structures. The observed structures indicate top-E shearing associated with folds with sub-horizontal axial planes affecting all units located west of the Vukanja Fault (Figs. 4h, 9a). This event is also associated with normal faults observed in all studied units (Fig. 4j). Field observations show ductile to brittle truncations or transitions west of the Vukanja Fault, which implies that deformation took place during exhumation. This agrees with field superposition criteria, which indicate that this deformation affected all previously described structures (e.g., Fig. 6f).

The shearing is rather large in the immediate footwall of the Vukanja Fault and occurred under lower-grade lower metamorphic conditions when compared with the older D1 event. Structures related to D5 shearing include a mylonitic foliation (S5), well-developed stretching lineations, together with shear-bands and sigma-clasts. These structures are obvious in the schists of the Boljevac - Vukanja sub-unit, in the migmatites of the Morava unit in the footwall of the Vukanja Fault and in the meta-sandstones of the Lomnica sub-unit (Figs. 6f, 7f–h). Retrograde metamorphism recorded by chloritization or grain-size reduction of mica is observed in the higher-grade metamorphic units. The stretching lineation dips gently in the same directions as the flanks of the dome, with kinematic indicators showing a general top-E sense of shear (Fig. 4g, orange arrows in Fig. 9a), deviating to top-NE or top-SE along its northern and southern flanks, respectively. This deformation was also coeval with the formation of decimetre- to metre-scale folds with sub-horizontal axial planes that affected an inherited steep foliations or previous fold generations (Figs. 4h, 5f–h, collapse folds, sensu Froitzheim et al., 1997).

At larger distances westwards from the Vukanja Fault, deformation decreases in intensity and gradually becomes more brittle, mylonitic structures being replaced by cataclastic shears and normal faults. Such normal faults also truncate D5 mylonites in the proximity of the Vukanja Fault, which is likely an effect of exhumation during deformation. These normal faults have various orientations across the dome (Fig. 5j), but generally accommodate a roughly E-W directed extension, which changes to more N-S oriented on the northern and southern flanks and dipping away from the dome (Fig. 6g,h). The normal faults were often tilted during the formation of the dome (Fig. 6h). These normal faults affect also the Miocene sediments surrounding the Jastrebac Mountains and are associated with syn-kinematic depositional features such as depositional fault breccia, footwall erosion and wedge-type deposition in book-shelf tilted geometries.

Several field observations suggest renewed small-scale contractional deformation during Pliocene - Quaternary times. A small number of reverse faults with several metres offsets and SW-ward vergence were observed in Quaternary sediments along the western and eastern part of Jastrebac Mountains. Locally, reverse faults thrust Mesozoic rocks over Miocene sediments (e.g., near the Vukanja village, Fig. 2). On the northern and southern flank of the mountains, Upper Pliocene - Quaternary coarse-clastic alluvial strata are thinning towards the mountains with 1-8° wedge slopes, the angle being higher on the southern slope of the mountains. This suggests an overall asymmetry of a Pliocene - Quaternary antiformal uplift. However, the available data are insufficient to clearly demonstrate such a structure and its genetic mechanisms in the Jastrebac Mountains.

4. Dating methods

Deriving thermochronological ages is critical for constraining the amounts and rates of exhumation created by various deformation events in the Morava and Jastrebac units. We have sampled a transect for low-temperature thermochronological dating (apatite and zircon fission tracks) by crossing the structure of the Jastrebac Mountains. This methodology is applied in the study of exhumation and cooling of rocks beneath ~250 °C (Tagami, 2005; Laslett et al., 1987). At the relatively small scale of the mountains, we have chosen 10 samples though to be representative for the differential exhumation of all units. The uncertainties in the existing Rb-Sr ages of the Ravnište pluton were corrected by a new LA-ICPMS U-Pb zircon age dating of one sample.

Among the 10 samples collected (~5 kg per location), seven yielded apatite fission track (AFT) and/or zircon fission track (ZFT ages) (Fig. 10). These samples are from a variety of lithologies (Figs. 2, 9, 10), which are gneisses (E17, E18, and E19) and micaschists of the Morava unit (JAS1), low degree cloritic-sericitic schists of the Boljevac - Vukanja sub-unit (JAS3,4), greenschist facies meta-sandstone of the turbiditic sequence flanking the central pluton (E16) and granodiorite sample of this pluton (E15). Apatite and zircon mineral separation, including crushing, sieving, heavy liquid and magnetic separation, followed standard procedures at VU Amsterdam (e.g., Foeken, 2004). While it was aimed to generate multiple age pairs (ZFT and AFT) for each sample this was not always possible, owing to the insufficient yield or poor quality of the apatite and zircon grains. Hence, six out of seven zircon samples and six out of seven apatite samples contained grains that could be used in further analysis. Zircon and apatite grains were mounted, grinded, polished, and etched. Apatite mounts were etched with 1.5 N HNO3 at 21 °C for 35 s, while the zircons grain mounts

Fig. 10. Dating results. a–f) Results of the apatite fission tracks analysis with single grain age distributions. n = number of grains counted; P — probability obtaining Chi-square (χ^2); D = dispersion in single grain ages; g–l) Results of the zircon fission tracks analysis with single grain age distributions. n = number of grains counted; P — probability obtaining Chi-square (χ^2); D = dispersion in single grain ages; The radial plots representing ZFT and AFT single grain age distributions were obtained using the TrackKey software (Dunkl, 2002). Grey lines indicate most prominent best-fit peaks, x and y axes show percentage of relative error and standard deviation. m) ^{238}U-^{206}Pb pooled crystallization age of sample JAS9.

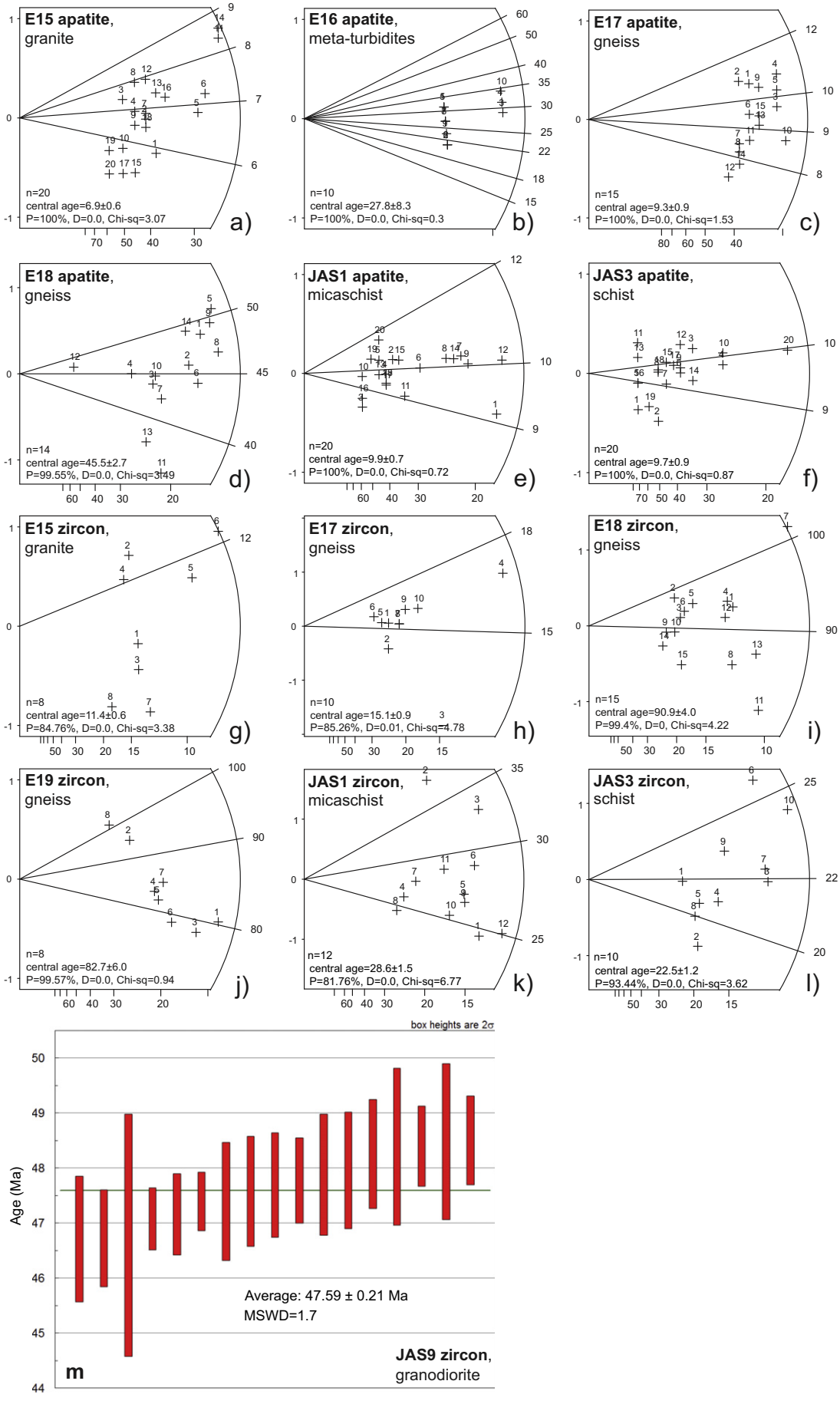
E15 apatite, granite
n=20
central age=6.9±0.6
P=100%, D=0.0, Chi-sq=3.07
a)
E16 apatite, meta-turbidites
n=10
central age=27.8±8.3
P=100%, D=0.0, Chi-sq=0.3
b)
E17 apatite, gneiss
n=15
central age=9.3±0.9
P=100%, D=0.0, Chi-sq=1.53
c)
E18 apatite, gneiss
n=14
central age=45.5±2.7
P=99.55%, D=0.0, Chi-sq=3.49
d)
JAS1 apatite, micaschist
n=20
central age=9.9±0.7
P=100%, D=0.0, Chi-sq=0.72
e)
JAS3 apatite, schist
n=20
central age=9.7±0.9
P=100%, D=0.0, Chi-sq=0.87
f)
E15 zircon, granite
n=8
central age=11.4±0.6
P=84.76%, D=0.0, Chi-sq=3.38
g)
E17 zircon, gneiss
n=10
central age=15.1±0.9
P=85.26%, D=0.01, Chi-sq=4.78
h)
E18 zircon, gneiss
n=15
central age=90.9±4.0
P=99.4%, D=0, Chi-sq=4.22
i)
E19 zircon, gneiss
n=8
central age=82.7±6.0
P=99.57%, D=0.0, Chi-sq=0.94
j)
JAS1 zircon, micaschist
n=12
central age=28.6±1.5
P=81.76%, D=0.0, Chi-sq=6.77
k)
JAS3 zircon, schist
n=10
central age=22.5±1.2
P=93.44%, D=0.0, Chi-sq=3.62
l)
box heights are 2σ
Age (Ma)
Average: 47.59 ± 0.21 Ma
MSWD=1.7
JAS9 zircon, granodiorite
m

were etched in a eutectic mixture of KOH and NaOH at 225 °C for 20 to 60 h. The etched mounts were attached against external mica detectors (EDM; Gleadow and Duddy, 1981) and irradiated at FRMII Garching (Technische Universität München, Germany). Zircon mounts were irradiated together with zircon age standards (Garver, 2003) and reference glass dosimeter CN-1, whereas apatite mounts were irradiated along with apatite age standards (Green, 1985) and reference glass dosimeter CN-5. The number of tracks in zircon and apatite grains and the external detectors were counted at the FT laboratory of VU Amsterdam (analyst P.A.M. Andriessen). Fission track ages are reported with statistical uncertainties quoted at the $\pm 1\sigma$ level, using zeta factor of 358 ± 10 (apatite, CN5 glass) and 128 ± 3 (zircon, CN1 glass) (see Fig. 10, Tables 1 and 2). The analysis also included the measurement of confined apatite fission track lengths and the etch pit diameters (Dpar) in order to define the kinetic characteristics of apatite grains (Donelick, 1993; Ketcham et al., 1999). Finally, the fission track ages were calculated using the TrackKey software (Dunkl, 2002). Homogeneity of the obtained single-grain ages within each sample was determined using the Chi-square (χ^2) test (Galbraith and Laslett, 1993). This test returns $P(\chi^2)$, the probability that the single-grain ages within the sample belong to the same population. The age population is homogeneous when $P(\chi^2) > 5\%$. In all cases, only a limited amount of confined apatite track lengths was measured that prevented making further inferences on their cooling or modelling cooling trajectories.

Zircon U-Pb geochronology was carried out on sample JAS9 at the University of Arizona. The rock was crushed, sieved to pass through 0.2 mm mesh and panned for primary removal of light minerals. Samples were then dried and passed through the Frantz isodynamic separator in 0.3 A current steps up to 1.2 A, to account for the magnetic susceptibility of zircon. This was followed by a separation step based on density, using heavy organic liquid methylene iodide (MI) of monitored 3.325 g/cm^3 density in which zircon crystals, with densities between 4.6–4.7 g/cm^3, sink. Igneous zircons were handpicked under a microscope, placed on double sided tape and mounted in epoxy. The zircon mount was then analyzed on a Nu Plasma instrument by multicollector laser-ablation-inductively coupled plasma–mass spectrometry (LA-ICPMS) at the Arizona LaserChron Center, following the procedures in Gehrels et al. (2008). In-run analysis of fragments of a large Sri Lanka zircon crystal (generally every fifth measurement) with known age of 564 ± 4 Ma (2σ error) is used for corrections (Gehrels et al., 2008). The uncertainty resulting from the calibration correction is generally ~1% (2σ) for both $^{206}Pb/^{207}Pb$ and $^{206}Pb/^{238}U$ ages. The reported ages are determined from the weighted mean of the $^{206}Pb/^{238}U$ ages of the concordant and overlapping analyses (Ludwig, 2005). The reported uncertainty is based on the scatter and precision of the set of $^{206}Pb/^{238}U$ or $^{206}Pb/^{207}Pb$ ages, weighted according to their measurement errors. The systematic error, which includes contributions from the standard calibration, age of the calibration standard, composition of common Pb and U decay constants, is generally ~1–2% (2σ).

4.1. Zircon U-Pb geochronology results

Thirty-seven core and rim individual U-Pb zircon determinations were carried out on sample JAS9 (Table 3). About half of the grains yielded different core and rim ages, with cores being older to significantly older than the rims. We interpret these older core grains to represent inherited grains in this magmatic sample. The inherited ages range from Archean - Proterozoic (3.2–2.4 Ga) to Neoproterozoic-Carboniferous (645–340 Ma) to some mid-Mesozoic (165–124 Ma) and late Mesozoic-early Cenozoic (70–60 Ma) (Table 3). No grain has particularly high U/Th ratios (>10) and, therefore, it is unlikely that any individual spot reflects a metamorphic event. Other cores as well as all rims yielded concordant Eocene ages, seventeen of which were pooled to determine an average $^{238}U/^{206}Pb$ age of 47.59 ± 0.21 Ma (MSWD = 1.7) (Table 3 and Fig. 10m). We interpret this age to represent the crystallization age of this plutonic rock.

4.2. Thermochronological results

All six samples used in ZFT analyses passed the Chi-square (χ^2) test, with values above 80% (Table 1, Fig. 10g–l). In addition, all six AFT samples also passed the Chi-square (χ^2) test, with values of 100%, thus confirming the homogeneity of the age populations (Table 2, Fig 10a–f). Mean apatite fission track lengths range between 11.68 ± 0.51 and 14.36 ± 0.84 μm, locally with a low number of very track lengths available. The average Dpar values are between 1.19 and 2.88 μm (Table 2). All samples parameters are detailed in Tables 1 and 2, while their central age and location is plotted in Fig. 9. Sample JAS1 yielded a ZFT central age of 28.6 ± 1.5 Ma, while the AFT central age of the same sample was 9.9 ± 0.7 Ma. Sample JAS3 yielded a ZFT central age of 22.5 ± 1.2 Ma, while the AFT central age is 9.7 ± 0.9 Ma. Sample E16 yielded a AFT central age of 27.8 ± 8.3 Ma, thus indicating cooling of the sample between ~120 °C and 60 °C during Late Oligocene times (AFT partial annealing zone, Laslett et al., 1987). Sample E17 yielded a ZFT central age of 15.1 ± 0.9 Ma and a AFT central age of 9.3 ± 0.9 Ma. East of the Vukanja Fault (Fig. 9), sample E18 yielded a ZFT central age of 90.9 ± 4.0 Ma, while the AFT central age was at 45.5 ± 2.7 Ma. The relatively short mean values of confined track measured (11.68 ± 0.51 μm, 17 tracks, Table 2) indicate an Eocene thermal overprint. The ZFT central age can be correlated with sample E19 that yielded a ZFT central age of 82.7 ± 6.0 Ma that indicates a similar cooling during the Late Cretaceous. Sample E15 in the Ravnište granodiorite yielded a ZFT central age of 11.4 ± 0.6 Ma and a AFT central age of 6.9 ± 0.6 Ma, while the two confined tracks measured have very high mean value of 14.36 ± 0.84 μm (Tables 1 and 2).

These results indicate a rather clear cooling history of all tectonic units in the Jastrebac Mountains. The Vukanja Fault separates two areas with different cooling histories (Fig. 9). All units west of this fault (i.e., Morava and Jastrebac, including the latter both sub-units) experienced a long period of late Oligocene - Miocene cooling. Given the much older 47.59 ± 0.21 Ma emplacement age of the Ravnište pluton, this cooling must reflect exhumation. In more detail, the cooling indicated by ZFT data is dispersed in the ~29–11 Ma interval. The marked differences across the Vukanja Fault infer differential tectonic exhumation. With the marked exception of sample E16, all other 4 AFT ages cluster in a narrow Late Miocene interval at ~10–6 Ma. When combined with the 45.5 ± 2.7 Ma AFT age of sample E18 immediately east and across the Vukanja fault, this infers differential tectonic exhumation. In contrast, sample E16 yielded an older ~28 Ma AFT age. This sample is situated in the contact metamorphic zone of the Ravnište pluton and is affected by large amounts of recrystallization indicating significant re-heating and observed fluid circulation along veins and dykes through the rock. It is possible that this sample was affected by a successive re-heating events and the central age obtained by the reduced number of apatites measured (10, Fig. 10) is a cumulative age rather than one exhumation age, significantly influenced by metasomatic fluid circulation (e.g., Luijendijk et al., 2011). Therefore, this sample was excluded from further interpretations. All other samples situated at larger distance from the pluton are certainly not affected by its thermal effects, as demonstrated by the rapid lateral decrease of metasomatism. In more detail, the distribution of ZFT data shows two different ages of 28.6 ± 1.5 and 15.1 ± 0.9 Ma in the immediate western footwall of the Vukanja Fault. At gradually farther distances westwards, the ZFT ages show again a different, but younger pair of 22.5 ± 1.2 and 11.4 ± 0.6 Ma. We interpret these differences to result from long residence times in the ZFT partial retention zone during the Oligocene – Miocene cooling, the areas situated at farther distances west-wards from the Vukanja Fault being exhumed slightly later than the immediate footwall. The cumulative exhumation during the Late Oligocene - Miocene times in the area west of the Vukanja fault should be in the order of 7 km, given the high value of present-day geothermal gradient of ~30 °C/km and ~200 °C temperature range of the ZFT and AFT partial annealing zones (Laslett et al., 1987; Tagami, 2005).

Table 1
Zircon fission track analytical data. All ages are central ages with 1σ standard error (Galbraith and Laslett, 1993). ρs (ρi) = spontaneous (induced) track densities; P (χ^2) = probability obtaining Chi-square (χ^2) for n degrees of freedom (n is number of crystals). Glass CN-1, Zeta 128 ± 3; all samples passed the Chi-sq. test at 5%.

Zircon FT analytical data								
Sample number	Rock type	Number of grains	ρ_d 10_6tr/cm^2 (N_d)	ρ_s 10_6tr/cm^2 (N_s)	ρ_i 10_6tr/cm^2 (N_i)	P(χ^2) (%)	Age dispersion (%)	Fission track age (Ma)
JAS3/4	Chloritic-sericitic schist	10	0.5184 (10704)	2.711 (797)	3.990 (1173)	93.4	0.00	**22.5 ± 1.2**
JAS1	Micaschist	12	0.5184 (10704)	4.002 (859)	4.631 (994)	81.7	0.00	**28.6 ± 1.5**
E15	Granodiorite	8	0.4719 (9744)	2.499 (715)	6.641 (1900)	84.7	0.00	**11.4 ± 0.6**
E17	Gneiss	10	0.4719 (9744)	2.689 (457)	5.361 (911)	85.2	0.01	**15.1 ± 0.9**
E18	Gneiss	15	0.4719 (9744)	7.403 (3120)	2.441 (1029)	99.4	0.00	**90.9 ± 4.0**
E19	Gneiss	8	0.4719 (9744)	5.587 (810)	2.028 (294)	99.5	0.00	**82.7 ± 6.0**

East of the Vukanja fault in its immediate hanging-wall area, two ZFT ages available indicate cooling during Late Cretaceous time ~94–80 Ma (Fig. 9). In the same area, the single apatite age available of 45.5 ± 2.7 Ma is, within error, in the range of the Ravnište pluton emplacement and its subsequent cooling.

Only a limited number of fission track lengths in apatite could be measured (Table 2), preventing further time-temperature modelling of the cooling paths (e.g., Ketcham et al., 2003). A careful analysis of low temperature thermochronological ages (Fig. 9) shows that exhumation was spatially distributed during the Late Oligocene - Miocene with ZFT and AFT ages situated in close spatial proximity. Such a distribution indicates a period of long lived exhumation at the scale of the entire dome and cannot discriminate tectonics from other exhumation processes. Therefore, time-temperature modeling was not performed and is not required. In contrast, tectonic exhumation during this period is clearly demonstrated by differential exhumation across the Vukanja Fault (Fig. 9a) and field structures, and is supported by the correlation with similar ages of tectonic exhumation of structures situated in the immediate vicinity of Jastrebac Mountains (see below).

5. Interpretation

The combined kinematic and thermochronological study of the Jastrebac Mountains area demonstrates a complex poly-phase evolution that is in partial agreement with previous, more qualitative inferences.

5.1. D1 shearing and Late Cretaceous exhumation near the contact between the Morava and Supragetic units

Constraining the significance of D1 shearing observed east of the Vukanja Fault is more difficult when compared with the rather clear subsequent events. D1 and D5 mylonites have a different metamorphic degree, but indicate a similar sense of shear, in average top-E. These D1 and D5 structures could not have formed during the same tectonic event because the Upper Cretaceous - Lower Paleogene protolith age of the Lomnica turbidites subsequently affected by the D5 extensional deformation is younger than the two Late Cretaceous ZFT exhumation ages (Cenomanian - lower Campanian within the error bars) located east of the Vukanja Fault, where higher temperature D1 mylonites occur. Furthermore, D1 greenschist-facies mylonites obviously post-date the Paleozoic deformation and peak amphibolite-facies metamorphic conditions, because they clearly truncate these earlier structures. Our observations of these relationships are unique, since the contact between the Serbo-Macedonian (i.e. Morava) unit and the Supragetic unit has very limited exposures elsewhere in Serbia. Given the spatial juxtaposition of D1 deformation and Late Cretaceous exhumation ages, interpreting a phase of Late Cretaceous tectonic exhumation associated with ~top-E shearing is appealing. However, this interpretation would be speculative if based solely on the data available in the study area, because the ~180 °C difference in cooling may also include other intervening tectonic or erosional processes.

There are two possibilities for interpreting the D1 shear zone at the contact between the Morava and Supragetic units. One possibility is that the shear zone reflects top-E intra-Morava thrusting near its overlying

Table 2
Apatite fission track analytical data. All ages are central ages with 1σ standard error (Galbraith and Laslett, 1993). ρs (ρi) = spontaneous (induced) track densities; P (χ^2) = probability obtaining Chi-square (χ^2) for n degrees of freedom (n is number of crystals); Std - standard deviation in track length distribution; Dpar - average etch pit diameter with its standard deviation. Glass CN-5, Zeta 358 ± 10; all samples passed the Chi-sq. test at 5%.

Apatite FT analytical data											
Sample number	Rock type	Number of grains	ρ_d 10_6tr/cm^2 (N_d)	ρ_s 10_6tr/cm^2 (N_s)	ρ_i 10_6tr/cm^2 (N_i)	P(χ^2) (%)	Age dispersion (%)	Fission track age (Ma)	Range of measured Dpar (# Dpar)	Mean track length (μm) /(#lengths)	Std (μm)
JAS3/4	Chloritic-sericitic schist	20	11.698 (24152)	0.087 (143)	1.885 (3084)	100	0.00	**9.7 ± 0.9**	1.19–1.55 (100)		
JAS1	Micaschist	20	11.698 (24152)	0.122 (234)	2.584 (4962)	100	0.00	**9.9 ± 0.7**	1.23–1.63 (100)	13.53 ± 1.44 (2)	1.02
E15	Granodiorite	20	10.537 (21755)	0.072 (139)	1.972 (3786)	100	0.00	**6.9 ± 0.6**	1.93–2.30 (100)	14.36 ± 0.84 (2)	1.18
E16	Meta-sandstone	10	10.537 (21755)	0.015 (13)	0.104 (88)	100	0.00	**27.8 ± 8.3**	1.56–2.88 (18)		
E17	Gneiss	15	10.537 (21755)	0.094 (130)	1.902 (2637)	100	0.00	**9.3 ± 0.9**	1.72–2.28 (71)	14.48 (1)	
E18	Gneiss	14	10.537 (21755)	0.372 (464)	1.537 (1918)	99.4	0.00	**45.5 ± 2.7**	1.89–2.25 (169)	11.68 ± 0.51 (17)	2.08

Table 3
U-Pb zircon geochronologic analyses of sample JAS09; C-analyses of zircon cores, R-analyses of zircon rims. Several zircon grains contain inherited cores. The distinct Eocene population at the lower age spectrum was used to determine the crystallization age.

Isotope ratios											Apparent ages (Ma)							
Analysis	U (ppm)	206Pb 204Pb	U/Th	206Pb* 207Pb*	± (%)	207Pb* 235U*	± (%)	206Pb* 238U	± (%).	error corr	206Pb* 238U*	± (Ma)	207Pb* 235U	± (Ma)	206Pb* 207Pb*	± (Ma)	Best age (Ma)	± (Ma)
DRH-JAS9-1	1711	17727	2,6	21,0981	4,3	0,0667	5,8	0,0102	4,0	0,68	65,5	2,6	65,6	3,7	69,3	101,2	65,5	2,6
DRH-JAS9-2	801	28655	3,2	21,4019	11,6	0,0522	11,9	0,0081	2,9	0,25	52,0	1,5	51,6	6,0	35,2	277,6	52,0	1,5
DRH-JAS9-3	210	11416	1,9	16,9258	11,6	0,1589	12,5	0,0195	4,6	0,37	124,5	5,7	149,8	17,4	570,1	254,0	124,5	5,7
DRH-JAS9-4R	555	9604	4,3	21,3432	8,7	0,0470	9,1	0,0073	2,4	0,27	46,7	1,1	46,6	4,1	41,8	208,9	46,7	1,1
DRH-JAS9-5C	1587	20738	2,6	20,6593	4,6	0,0489	4,8	0,0073	1,2	0,25	47,1	0,6	48,5	2,3	119,1	109,5	47,1	0,6
DRH-JAS9-6R	972	31054	2,6	21,3321	8,8	0,0559	9,0	0,0086	1,8	0,20	55,5	1,0	55,2	4,9	43,0	211,8	55,5	1,0
DRH-JAS9-8R	1610	14916	1,6	20,7620	4,3	0,0490	4,5	0,0074	1,1	0,25	47,4	0,5	48,6	2,1	107,4	102,5	47,4	0,5
DRH-JAS9-10R	1285	17726	2,7	21,5006	6,6	0,0483	6,8	0,0075	1,5	0,22	48,4	0,7	47,9	3,2	24,2	158,1	48,4	0,7
DRH-JAS9-11C	919	14822	1,7	20,9436	7,8	0,0615	8,4	0,0093	3,2	0,38	60,0	1,9	60,6	5,0	86,8	185,3	60,0	1,9
DRH-JAS9-12R	2011	21753	2,5	20,9832	3,5	0,0494	4,0	0,0075	2,1	0,51	48,2	1,0	48,9	1,9	82,3	82,6	48,2	1,0
DRH-JAS9-13C	773	17037	2,9	22,7085	17,1	0,0509	18,0	0,0084	5,4	0,30	53,8	2,9	50,4	8,8	-108,6	424,1	53,8	2,9
DRH-JAS9-14R	3531	48541	5,8	20,5837	1,8	0,0527	2,9	0,0079	2,3	0,79	50,6	1,2	52,2	1,5	127,7	41,9	50,6	1,2
DRH-JAS9-15C	1891	45022	2,4	21,5913	4,4	0,0482	4,7	0,0076	1,7	0,35	48,5	0,8	47,8	2,2	14,0	107,0	48,5	0,8
DRH-JAS9-16R	1567	13841	3,7	20,1761	4,8	0,0516	5,6	0,0075	2,9	0,52	48,5	1,4	51,1	2,8	174,6	110,9	48,5	1,4
DRH-JAS9-17C	576	92367	5,1	18,7987	1,5	0,3983	1,8	0,0543	1,1	0,59	340,9	3,6	340,4	5,3	337,1	33,7	340,9	3,6
DRH-JAS9-18R	1233	11266	3,6	22,3526	11,8	0,0324	12,0	0,0053	1,7	0,15	33,8	0,6	32,4	3,8	-69,9	289,7	33,8	0,6
DRH-JAS9-19C	885	5754	2,5	21,5140	13,3	0,0544	13,7	0,0085	3,3	0,24	54,5	1,8	53,8	7,2	22,7	320,2	54,5	1,8
DRH-JAS9-20R	1034	16702	3,3	22,8152	11,2	0,0455	11,5	0,0075	3,0	0,26	48,4	1,4	45,2	5,1	-120,2	275,9	48,4	1,4
DRH-JAS9-21C	775	15447	1,8	20,8737	4,8	0,1467	5,7	0,0222	3,0	0,53	141,6	4,2	139,0	7,4	94,7	114,4	141,6	4,2
DRH-JAS9-22R	1239	31603	4,0	21,0987	4,7	0,0487	5,2	0,0075	2,3	0,44	47,9	1,1	48,3	2,5	69,2	111,0	47,9	1,1
DRH-JAS9-23C	55	59637	1,9	3,9854	0,8	16,9495	3,8	0,4899	3,7	0,98	2570,3	77,9	2932,0	36,1	3190,5	12,5	3190,5	12,5
DRH-JAS9-24R	1214	22851	3,1	21,5734	7,5	0,0472	7,8	0,0074	2,3	0,29	47,4	1,1	46,8	3,6	16,0	180,0	47,4	1,1
DRH-JAS9-25C	193	1090	3,5	19,2645	14,0	0,1916	15,1	0,0268	5,6	0,37	170,3	9,5	178,0	24,6	281,4	321,3	170,3	9,5
DRH-JAS9-26R	1361	30092	2,9	20,9578	4,0	0,0488	4,5	0,0074	2,0	0,44	47,7	0,9	48,4	2,1	85,2	95,3	47,7	0,9
DRH-JAS9-27C	489	3521	5,4	23,5818	13,5	0,0640	13,9	0,0109	3,3	0,24	70,2	2,3	63,0	8,5	-202,4	340,2	70,2	2,3
DRH-JAS9-28R	1174	11461	3,0	21,9874	11,1	0,0460	11,2	0,0073	1,6	0,14	47,2	0,7	45,7	5,0	-29,8	269,4	47,2	0,7
DRH-JAS9-29C	1144	5392	9,3	19,5234	5,5	0,1246	6,2	0,0176	2,9	0,46	112,8	3,2	119,3	7,0	250,7	127,6	112,8	3,2
DRH-JAS9-30R	1325	13454	3,2	22,3172	8,0	0,0449	8,2	0,0073	1,9	0,23	46,7	0,9	44,6	3,6	-66,0	195,6	46,7	0,9
DRH-JAS9-31C	270	17683	2,0	19,8032	10,7	0,1802	11,1	0,0259	2,9	0,26	164,7	4,7	168,2	17,2	218,0	248,7	164,7	4,7
DRH-JAS9-32R	1188	22579	2,6	21,5633	12,2	0,0474	12,4	0,0074	2,1	0,17	47,6	1,0	47,0	5,7	17,1	293,6	47,6	1,0
DRH-JAS9-33C	1578	42493	1,8	14,4770	0,5	1,0034	8,5	0,1054	8,4	1,00	645,7	51,9	705,5	43,1	901,0	11,3	645,7	51,9
DRH-JAS9-34R	1391	19194	2,9	20,6229	4,6	0,0499	5,1	0,0075	2,2	0,43	48,0	1,1	49,5	2,5	123,2	108,2	48,0	1,1
DRH-JAS9-35C	1410	73588	3,6	6,5163	3,1	2,6624	27,6	0,1258	27,5	0,99	764,0	198,0	1318,1	206,9	2384,8	53,0	2384,8	53,0
DRH-JAS9-36R	3438	4313	3,5	19,8832	7,9	0,0548	7,9	0,0079	0,8	0,11	50,7	0,4	54,2	4,2	208,6	182,3	50,7	0,4
DRH-JAS9-37C	729	63742	2,8	15,0092	0,7	0,8320	4,1	0,0906	4,0	0,99	558,9	21,4	614,7	18,7	826,1	14,0	558,9	21,4
DRH-JAS9-38R	1146	24257	3,1	21,3290	13,1	0,0481	13,2	0,0074	1,6	0,12	47,8	0,8	47,7	6,1	43,4	313,2	47,8	0,8
DRH-JAS9-39C	188	2001	2,3	18,7836	15,0	0,1658	16,6	0,0226	7,0	0,42	144,0	10,0	155,8	23,9	338,9	341,4	144,0	10,0
DRH-JAS9-40R	1297	1826	2,4	19,9086	12,9	0,0504	13,8	0,0073	4,7	0,34	46,8	2,2	50,0	6,7	205,6	301,1	46,8	2,2

contact with the Supragetic. In this hypothesis, the shear zone was originally dipping W-wards and was subsequently tilted by footwall uplift against the later detachment (see below). In this hypothesis, such an out-of-sequence thrusting was Late Cretaceous or older and the exhumation was assisted by erosional breakdown during or after thrusting. This hypothesis is not supported by our field data because all observed contractional structures post-date the shear zone by either refolding or truncating D1 structures. The second possibility is that the contact between the Morava and Supragetic units is a Late Cretaceous detachment (DEF shear zone Figs. 2 and 9) that formed in its footwall the wide shear zone affecting the Morava unit above the Vukanja Fault. In this situation, the ZFT ages would represent direct tectonic exhumation of an extensional footwall.

5.2. Latest Cretaceous - Eocene contraction and emplacement of the Ravnište pluton

The successive D2-D4 phases form together a larger tectonic event that thrusted the Morava over the Jastrebac unit (the MJ contact area in Figs. 2 and 9), expressed by burial, shearing, metamorphism and continued contraction. Furthermore, the metamorphosed sedimentary and mafic Boljevac - Vukanja sub-unit was thrust over the low-degree metamorphosed coarse-grained turbidites of the Lomnica sub-unit (the BVL contact area in Figs. 2 and 9).

The intensity of D3 shearing was high in the meta-sediments of the Lomnica and in the upper parts of the Boljevac-Vukanja unit, implying a proximal position in the footwall of the main nappe contact at the time of burial. The contrasting metamorphic degree of the two Jastrebac tectonic sub-units indicates that their thrusting superposition post-dated the initial stage of burial and metamorphism. This implies that the initial burial metamorphism took place in response to nappe stacking along the MJ contact and was subsequently followed by thrusting along the BVL contact (Figs. 2 and 9). The geometry of the upright folds (D4) observed in all units of the Jastrebac Mountains is similar with the larger scale antiform that contains in its core the central Ravnište intrusion (Fig. 9b). This implies that the phase of upright folding (D4) was still on-going during the Eocene emplacement of the Ravnište pluton at ~47 Ma.

The overall D2-D4 contraction took place during latest Cretaceous - Middle Eocene times, as demonstrated by the combination of our observations with structural and burial constraints available in the western adjacent Sava Zone and Kopaonik structure (Fig. 1b, see also Schmid et al., 2008; Schefer et al., 2011). This age is also in agreement with previous studies of the Jastrebac Mountains (Grubić, 1999; Marović et al., 2007). Similar to these studies, we conclude that this shortening was coeval with the deposition of the coarse-grained syn-kinematic trench turbidites that were buried, metamorphosed and subsequently exhumed in the Lomnica unit.

This major event of contraction did not create major exhumation in the studied area of the Serbo-Macedonian unit. Although our data are limited, this event did not reset the ZFT exhumation ages and is, possibly, reflected only in single obtained AFT age of ~45 Ma. However, this age is very close to the timing of the Ravnište pluton emplacement

(~47 Ma). Therefore, the AFT system could have been thermally reset by this emplacement and subsequent cooling. Such caution is advised due to the structural position of the sample E18 (Fig. 9) that, after restoring the Miocene offset along the Vukanja detachment, could have been in spatial proximity of the pluton at the time of its emplacement.

5.3. Late Oligocene - Miocene extension and exhumation of the dome

Our combined kinematic and low temperature thermochronological data demonstrate a novel stage of Late Oligocene - Miocene extensional deformation and associated exhumation in the Jastrebac Mountains. The D5 shearing in average greenschist-facies metamorphic conditions created the Vukanja detachment and changed gradually to cataclastic and brittle normal faulting during the extensional exhumation of its footwall. Ductile kinematic indicators indicate a top-E transport direction, somewhat diverging along the northern and southern flanks of the dome. The normal faults may have larger offsets, such as along the western flank of the dome where they truncate the ophiolites and ophiolitic melange together with the overlying Lower Cretaceous sediments (Fig. 9b). The Vukanja Fault hanging-wall recorded brittle normal faulting during this deformation. Extension was also associated with D5 folds with horizontal axial planes indicating accompanying vertical flattening. All these structures are similar with other observations in orogenic extensional domes controlled by major detachments (e.g., Coletta and Angelier, 1982; Wernicke, 1985; Buck et al., 1988; Brun and Sokoutis, 2007 and references therein).

Field observations and, partially, the distribution of ZFT and AFT ages show that extensional deformation reactivated the thrust contact between the Morava and Jastrebac units (MJ contact, Fig. 9), possibly facilitated by the inherited weakness of this suture zone. Extensional deformation also affected the Morava unit by intense shearing in the footwall of the Vukanja Fault. The age of the extensional event is demonstrated by the long stage of cooling (~29–6 Ma) observed in the combined ZFT and AFT data located in the footwall of the Vukanja detachment (Fig. 9) and by the clear tectonic omission observed when compared with the ZFT and AFT data of its hanging-wall. ZFT ages of ~28–15 Ma in the immediate footwall of the Vukanja Fault imply that the initial Late Oligocene - Early Miocene exhumation was slow and accelerated during the Middle-Late Miocene. This is also in agreement with the limited information available on fission track length analysis. When compared with the typical thermal and isostatic re-equilibration of such extensional structures (e.g., Wernicke, 1985), this means that most of the dome geometry of the Jastrebac Mountains was acquired during the Middle-Late Miocene stages of extension.

The extension was likely followed by a period of Pliocene - Quaternary contraction that accentuated the central antiform of the Jastrebac Mountains with uplift in the order of maximum few hundred metres. However, our limited data are not able to properly discriminate between the breakdown of a morphology built up until the Late Miocene from a subsequent event of contraction.

6. Discussion

Our data and interpretation are in general agreement with observations in other areas situated near the Sava suture zone in the Dinarides, either in European-derived or in Dinaridic units. Contraction during latest Cretaceous - Eocene times was similarly documented in many other places of the Dinarides, including in or near the Sava Zone (e.g., Schmid et al., 2008; Ustaszewski et al., 2010; Schefer et al., 2011; Toljić et al., 2013; van Gelder et al., 2015). These studies have shown that almost all these areas experienced a period of latest Cretaceous contraction recorded in distal Adriatic units overlaid by the turbidites of the Sava suture zone. Our observations agree with these studies, which showed that contraction took place in a similar sequence of burial and metamorphism, asymmetric top W, SW or S shearing and upright folding associated or not with the emplacement of coeval plutons.

Along the strike of the Sava Zone, the previously buried and metamorphosed distal Adriatic margin was subsequently exhumed by many Oligocene - Miocene detachments forming extensional domes in their footwall that had a clear preference for reactivating the inherited weakness of the Sava zone turbidites. Such situations are observed for instance along the Dinaridic strike in the Medvednica Mountains of Croatia (van Gelder et al., 2015), Kosara-Prosara-Motajica system of Bosnia and Herzegovina and Croatia (Ustaszewski et al., 2010), Fruška Gora, Cer and Bukulja Mountains of northern and Central Serbia (Fig. 1b, Stojadinović et al., 2013; Toljić et al., 2013), in the adjacent area of the Kopaonik - Studenica (Fig. 1b, Schefer et al., 2011), as well as buried beneath the Miocene sediments of the Pannonian Basin (Matenco and Radivojević, 2012). The peak of extension in all these areas is always around 15–11 Ma, while the onset of extension is still unclear. Challenging the previous postulations that the onset of extension in the larger Pannonian basin at ~20 Ma (e.g., Horváth et al., 2006), more recent studies have inferred an earlier Oligocene onset of extension (~28 Ma), based on one set of high-temperature thermochronological data (high resolution Rb-Sr, Toljić et al., 2013) and on the emplacement of genetically-related plutons in the footwall of detachments (i.e. Bukulja pluton at ~23 Ma , Stojadinović et al., 2016). Our study confirms this earlier onset of extension at ~28 Ma in the Jastrebac Mountains area situated in the Morava corridor prolongation of the Pannonian basin.

6.1. Towards defining a Late Cretaceous detachment at the Morava/Supragetic contact

Among the two possible interpretations of the D1 top-E shearing, the one of a Late Cretaceous detachment exhuming the Morava unit from beneath the Supragetic hanging-wall is supported by other regional information outside the study area. The nappe contact between the low-degree metamorphics of the Supragetic unit and its Getic nappe footwall made up by Triassic - Lower Cretaceous sediments (mostly carbonates) is exposed immediately east of the Morava river (Fig. 1b,c). Along its very long strike spanning from the South Carpathians of Romania to SW Bulgaria (Fig. 1b), this Supragetic/Getic contact is interpreted as a late Early Cretaceous contact (intra-Albian, ~110–100 Ma), which is the timing of the onset of continental collision following subduction of the Ceahlau-Severin ocean in the Carpatho-Balkanides (e.g., Schmid et al., 2008), followed by the continuation of collision during the latest Cretaceous times. This is demonstrated by post-tectonic covers, burial metamorphism and provenance studies (e.g., Iancu et al., 2005; Kounov et al., 2010; Neubauer and Bojar, 2013 and references therein). Our preliminary observations east of the Morava river show a brittle thrust contact that does not appear to be related to the major shear zone observed in the Morava unit of the Jastrebac Mountains.

The highest structural position of Serbo-Macedonian unit when compared with other European-derived units is generally postulated on their higher metamorphic degree and assumed structural geometries (see discussion in Schmid et al., 2008; Matenco and Radivojević, 2012), but no published kinematic studies are available for a correlation in the very few areas where their contact is exposed in Serbia. South of our area, a thermochronological study conducted in the Serbo-Macedonian units of SE Serbia and adjacent countries has yielded ZFT ages interpreted to reflect a period of post-orogenic extension (relative to the Carpatho-Balkanides orogen) and formation of extensional detachments ~110–90 Ma (Antić et al., 2016b). Given the large uncertainties in their ZFT ages (error bars of 15 Ma in average), data from this study agrees with the hypothesis of an extensional detachment in the Jastrebac Mountains. Furthermore, our preferred hypothesis also agrees with other similar indications of Late Cretaceous extension located in similar positions in the vicinity of the Sava suture zone to the north and NE. Widespread Turonian - early Campanian normal faulting associated with bi-modal magmatism at ~85 Ma is observed in the Upper Cretaceous cover of the Serbo-Macedonian unit in the area of Belgrade

(Fig. 1b, Toljić, 2006). Further westwards, a Late Cretaceous extensional detachment (~82 Ma) is observed in the internal Dinarides units in the Medvednica Mountains (near Zagreb, Croatia), correlated to the Gosau extension and associated sedimentation of the Eastern Alps (van Gelder et al., 2015). To the NE, E and SE of our area, the long Apuseni - Banat - Timok - Panagyurishte - Srednogorie magmatic belt (~92–67 Ma) formed in response to the Neotethys subduction system of the Dinarides - Hellenides and was associated with widespread extension, well studied in the neighbouring Timok zone of Serbia (e.g., von Quadt et al., 2005; Gallhofer et al., 2015 and references therein). Although these studies do not always agree on the responsible geodynamic context and exact location with respect to the plate margin, it is rather clear that a period of Late Cretaceous extension (~90–80 Ma) affected regions situated near the Sava suture zone. Therefore, the existence of a Late Cretaceous extensional detachment in the Jastrebac Mountains is our preferred interpretation in the regional geodynamic context. However, the alternative hypothesis of out-of-sequence Late Cretaceous or older thrusting of the Supragetic over the Serbo-Macedonian cannot be completely discarded given the limited available information.

6.2. The affinity of the Jastrebac unit and tectonic reversal of its sub-units

The metamorphosed sequence of the Jastrebac unit (Fig. 3) is similar to other sequences in the exhumed distal Adriatic margin, overlying ophiolites and metamorphosed sediments of the Sava suture zone. The uppermost Cretaceous (-Lower Paleogene?) meta-turbidites of the Lomnica unit affected by gradually increasing metasomatism towards the central Ravniště pluton can be correlated with the deep water syn-contractional trench turbidites and pelagic deposition of similar age observed elsewhere in the Sava Zone, taking into account that the suture zone in the Jastrebac Mountains was buried deeper and exhumed by the subsequent extensional uplift in the core of a large dome (Figs. 1c, 9b, see also Schmid et al., 2008). Immediately west of our study area, such sediments outcrop on the eastern flank of the Kopaonik Mountains (Fig. 11), where more pelagic sediments intercalated with ophiolitic detritus are observed (the Scaglia Rossa with ophiolitic detritus of Schmid et al., 2008; Schefer, 2010). The coeval coarse-grained meta-turbidites of the Lomnica unit are the more proximal trench equivalent of these sediments, buried deeper by the thrusting of the overlying Serbo-Macedonian margin.

The metamorphosed melange observed in the Boljevac-Vukanja unit is an obvious metamorphosed equivalent of the ophiolitic melange, which is widely observed elsewhere beneath the Western Vardar ophiolites (Fig. 3). Beneath this melange, the metamorphic sequence is equivalent to the non-metamorphic sedimentary succession indicating the gradual deepening of the distal Adriatic unit since Middle-Late Triassic times. The key in the interpretation are the calcschists intercalated in the marbles to quartzitic sequence observed in the Boljevac-Vukanja unit. In the neighbouring Studenica and Kopaonik window (Fig. 1), similar calcschists (i.e. the Kopaonik formation, metamorphosed deep water limestones and calciturbidites), were dated as Upper Triassic and interpreted to represent the deepening from shallow water limestones to radiolarites recognized in their protolith (Schefer et al., 2010). At farther distances from our study area, similar calc-schists of the Fruška Gora Mountains were interpreted as late Middle Triassic, implying an earlier onset of the deepening in a more distal position along the passive continental margin. This event of deepening post-dated the late Anisian continental rifting and associated magmatism (Toljić et al., 2013, see also Pamic, 1984; Dimitrijević, 1997). Given the observation that the Boljevac - Vukanja unit is in a more distal position on the former Adriatic passive continental margin when compared with the Kopaonik dome (Fig. 11), we speculate that the calc-schists in the studies area are late Middle Triassic (Ladinian) in age (Fig. 3). In this hypothesis, the overlying quartzites would be metamorphosed Upper Triassic - Middle Jurassic radiolarites, while the underlying marbles and actinolite-bearing schists would represent the equivalent of the Lower - Middle Triassic clastic-carbonatic sequence containing rifting-related volcanics (Fig. 3). Such a speculation is in line with the lateral variability in the age of rifting and thermal subsidence of the Adriatic passive continental margin observed elsewhere in the Dinarides (e.g. Pamic, 1984; Missoni et al., 2012).

The uppermost Cretaceous turbidites of the Sava suture zone outside our study area are in an intermediate tectonic position, being tectonically overlain by the European-derived margin (i.e. the Serbo-Macedonian/Morava unit) and thrust over or otherwise overlying the former Adriatic margin (i.e., the Jadar-Kopaonik unit near the study area, Fig. 1b). In our study area, the metamorphosed equivalents of these turbidites in the Lomnica unit are in the lowermost structural position, beneath the metamorphosed Adriatic equivalents of the Boljevac - Vukanja unit. This relates to the sequence of thrusting that buried deeper the higher degree metamorphosed rocks of the Boljevac - Vukanja unit with respect to the Lomnica unit. Their thrust contact (BVL in Fig. 9) is obviously an out-of-sequence thrust formed later during the Late Cretaceous - Eocene contraction.

6.3. Kinematics of extension

The first-order similarities of contractional and subsequent extensional deformation described in this paper with the deformation documented elsewhere become obvious when constructing a regional cross-section

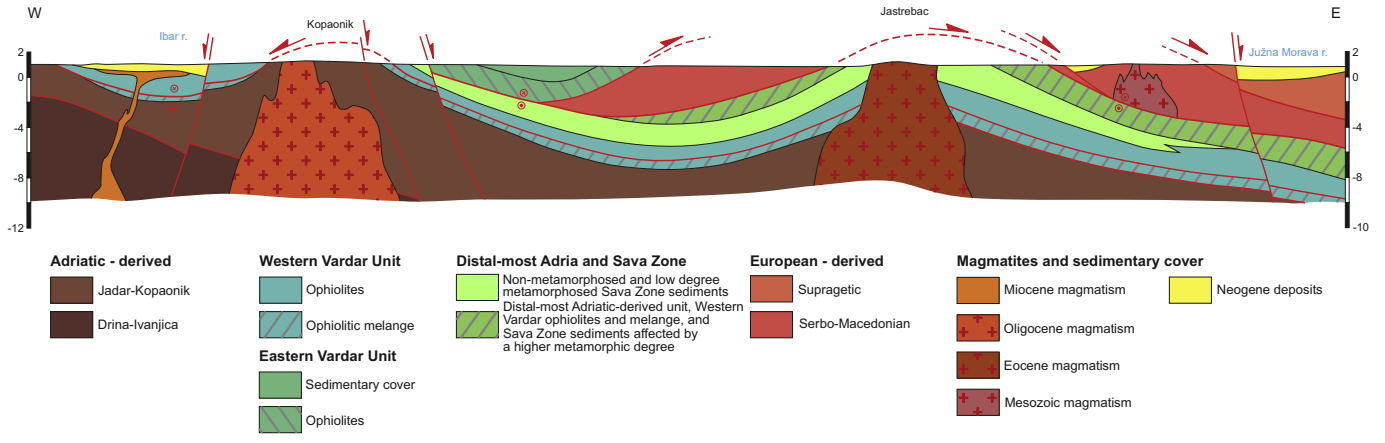

Fig. 11. Regional tectonic cross section combining the structure of the Kopaonik window (from Schefer, 2010) with structure of the Jastrebac dome derived from the results of the present study. Note that the main extensional shearing in the Kopaonik window is top-N and the E-W extension in the same area is minor. In comparison the main extensional shearing in the Jastrebac dome is top-E, while the effects of one other N-S oriented extensional deformation cannot be properly depicted, but are certainly minor. Note that the inclination of Sava Suture sediments at depth is lower when compared with Fig. 1c, accounting for the low amount of exhumation derived by our study in the Lomnica unit.

linking our tectonic interpretation with the one in the neighbouring Kopaonik structure along a regional cross-section (Fig. 11, see also Cvetkovic et al., 2004; Schefer, 2010; Schefer et al., 2011; Mladenović et al., 2015 and references therein). Both structures are similarly-sized extensional domes that expose the rocks previously buried and metamorphosed during the latest Cretaceous - Eocene contraction. Both domes expose in their core intrusions of granodioritic-average composition, although their age and composition is slightly different (~30 Ma and more crustal rich with a higher variability in the case of Kopaonik).

The main transport directions for the Oligocene - Miocene extensional deformation controlled by detachments in the Dinarides range roughly from top-N to top-E (Matenco and Radivojević, 2012; van Gelder et al., 2015 and references therein). Although both N-S and E-W extensional directions have been observed from normal faulting in the Kopaonik window and interpreted as two distinct deformation events (Schefer, 2010; Mladenović et al., 2015), the main transport direction there is top-N (possibly also top NNE) at ~16–11 Ma, accommodating the formation of the northern Miocene Kraljevo Basin (Fig. 1b). The comparison with our study area of the Jastrebac Mountains (Fig. 11) shows that the main direction of tectonic transport changes rapidly on a distance of ~40 km from top-N (Kopaonik) to top-E (Jastrebac), with significant spread in the direction of deformation in both areas. This correlation shows that kinematic changes are related rather to the spatial variability of deformation than to superposition of separate events with time. Structural and geodynamic studies have demonstrated that the extension in the southern part of the Pannonian Basin is controlled by the large-scale clockwise rotation of the Tisza-Dacia unit (roughly the Romanian Carpathians and their southern prolongation, Fig. 1) during the Miocene subduction roll-back of a slab attached to the European continent (e.g., Horváth et al., 2015). The pole of this rotation controlling the amount and direction of extension is situated somewhere south of the Jastrebac Mountains at the neighbouring termination of the Miocene Morava Basin (Fig. 1a, see also Matenco and Radivojević, 2012). Significant variability of the deformation direction is expected near any pole of rotation around a vertical axis, such as observed in the extensional kinematics of the Rhodope core-complex (Brun and Sokoutis, 2007). Our correlation (Fig. 11) infers that the Kopaonik structure was situated more west of this rotational pole, which facilitated the dominant top-N-NE direction of tectonic transport during extension (Fig. 1a). In contrast, the Jastrebac Mountains were situated north of this rotational pole and were, therefore, subjected to the main top-E direction of tectonic transport. Any horizontal shift in the position of the rotational pole during the long-lived extension could have created significant changes in extensional direction in such close proximity to the pole. Adding to this complexity, exhumation of extensional domes is known to create a variability in the orientation of normal faults at their along-strike terminations. In such complex extensional settings, it is rather clear that large offset structures, such as detachments, are far more indicative for the regional deformation when compared with low offset structures, such as brittle normal faults. The latter can yield almost any direction of extension in large-scale extrapolations near such rotational poles.

7. Conclusions

Our combined structural and thermochronological study of the Jastrebac Mountains area of the Dinarides chain has documented a poly-phase tectonic evolution that was responsible for the orogenic build-up, extensional collapse in the forearc during subduction and large scale back-arc extension situated in the proximity of a rotational pole. The Jastrebac Mountains expose a large-scale top-E shear zone responsible for the Late Cretaceous exhumation of their eastern flank. The most likely interpretation of this shear zone is a Late Cretaceous extensional detachment creating the observed separation between the high-grade metamorphism of the Serbo-Macedonian unit in the footwall and the weakly metamorphic Supragetic nappe in the hanging-wall. This type and age of deformation was recently described in other neighbouring areas situated in similar tectonic positions along the Dinaridic strike and are related to the extension recorded in the fore-arc basement and its overlying cover during the Late Cretaceous subduction of the Neotethys Ocean (see also Antić et al., 2016b; Toljić, 2006).

Similar to observations recorded elsewhere, the extensional event was followed by a period of latest Cretaceous - Eocene contraction and magmatic emplacement during the continental collision between European- and Adriatic-derived units. In the Jastrebac Mountains, this is observed by successive events of burial and metamorphism, top-W shearing and asymmetric folding, and upright folding coeval with the emplacement of the central pluton. The tectonic inversion observed in the central Jastrebac unit is an effect of a late-stage, most likely out-of-sequence thrust that truncated the earlier buried Adriatic units and Sava suture zone turbidites.

This was followed by the activation of a second extensional detachment during a Late Oligocene - Miocene event of extension related to the opening of the larger Pannonian Basin located northwards. The extension exhumed the previously buried and metamorphosed Adriatic units and sediments of the Sava suture zone in the core of an extensional dome that formed in the footwall of a large detachment. This detachment reactivated pre-existing nappe contacts and created a wide shear zone in the hanging-wall Serbo-Macedonian unit. The eastern limit of this shear zone is clearly expressed by a tectonic omission observed between the footwall and hanging-wall of the Vukanja Fault in our thermochronological data. The proximity of our study area to the pole of vertical-axis rotation that accompanied the overall extension in the southern Pannonian Basin produced a variability of extensional directions observed in the transect across the strike of the Dinarides and their contact with the Carpathians. One other effect of the proximity to the rotational pole is the long-lived period of extension that started at low rates during Late Oligocene - Early Miocene and accelerated during Middle - Late Miocene.

Acknowledgements

This study is a result of the collaboration between Utrecht University, The Netherlands and Faculty of Mining and Geology, University of Belgrade, Serbia and was funded by the Netherlands Research Centre for Integrated Solid Earth Science (ISES). This study was partly supported by the Ministry of Education, Science and Technological Development of the Republic of Serbia, Projects No. 176015 and No. 176019. The detailed comments and suggestions of Marko Vrabec, Jan Pleuger, Alexandre Kounov and an anonymous reviewer are gratefully acknowledged. The positive understanding of Editors in handling our manuscript is very much appreciated. Stefan Schmid and Kamil Ustaszewski are acknowledged for discussions in understanding the evolution of the Dinarides. Vladica Cvetković is gratefully acknowledged for long discussions on the Dinarides magmatism, his permanent support and help in developing petrological interpretations. Jane Chadwick is acknowledged for discussions on understanding magmatism and geochemical interpretations.

References

Antić, M., Peytcheva, I., von Quadt, A., Kounov, A., Trivić, B., Serafimovski, T., Tasev, G., Gerdjikov, I., Wetzel, A., 2016a. Pre-Alpine evolution of a segment of the North-Gondwanan margin: Geochronological and geochemical evidence from the central Serbo-Macedonian Massif. Gondwana Res. 36, 523–544.

Antić, M.D., Kounov, A., Trivić, B., Wetzel, A., Peytcheva, I., Quadt, A., 2016b. Alpine thermal events in the central Serbo-Macedonian Massif (southeastern Serbia). Int. J. Earth Sci. 105:1485. http://dx.doi.org/10.1007/s00531-015-1266-z.

Balázs, A., Matenco, L., Magyar, I., Horváth, F., Cloetingh, S., 2016. The link between tectonics and sedimentation in back-arc basins: new genetic constraints from the analysis of the Pannonian Basin. Tectonics 35, 1526–1559.

Brun, J.-P., Faccenna, C., 2008. Exhumation of high-pressure rocks driven by slab rollback. Earth Planet. Sci. Lett. 272, 1–7.

Brun, J.-P., Sokoutis, D., 2007. Kinematics of the Southern Rhodope Core Complex (North Greece). Int. J. Earth Sci. 96, 1079–1099.

Brun, J.-P., Sokoutis, D., 2010. 45 m.y. of Aegean crust and mantle flow driven by trench retreat. Geology 38, 815–818.

Buck, W.R., Martinez, F., Steckler, M.S., Cochran, J.R., 1988. Thermal consequences of lithospheric extension: pure and simple. Tectonics 7, 213–234.

Červenjak, Ž., Ferara, G., Tongiorgi, E., 1963. Age determination of some Yugoslav granites and granodiorites by the rubidium-strontium method. Nature 197, 893.

Chiari, M., Djerić, N., Garfagnoli, F., Hrvatović, H., Krstić, M., Levi, N., Malasoma, A., Marroni, M., Menna, F., Nirta, G., Pandolfi, L., Principi, G., Saccani, E., Stojadinović, U., Trivić, B., 2011. The geology of Zlatibor-Maljen area (western Serbia): a geotraverse across the ophiolites of the Dinaric - Hellenic collisional belt. Ofioliti 36, 139–166.

Coletta, B., Angelier, J., 1982. Sur les systemes de blocs failles bascules associes aux fortes extensions: etude preliminaire d'exemples ouestamericains (Nevada, USA et Basse California, Mexique). Academie de Sceances Compte Rendus 294, 467–469.

Cvetković, V., Knezevic, M., Pecskay, Z., 2000. Tertiary igneous formations in the Dinarides, Vardar zone and adjacent regions: from recognition to petrogenetic implications. In: Karamata, S., Jankovic, S. (Eds.), Geology and Metallogeny of the Dinarides and the Vardar Zone The Academy of Science and Arts of the Republic of Srpska, Banja Luka, pp. 245–253.

Cvetkovic, V., Prelevic, D., Downes, H., Jovanovic, M., Vaselli, O., Pécskay, Z., 2004. Origin and geodynamic significance of Tertiary postcollisional basaltic magmatism in Serbia (Central Balkan Peninsula). Lithos 73, 161–186.

Cvetković, V., Šarić, K., Prelević, D., Genser, J., Neubauer, F., Höck, V., von Quadt, A., 2013. An anorogenic pulse in a typical orogenic setting: the geochemical and geochronological record in the East Serbian latest Cretaceous to Palaeocene alkaline rocks. Lithos 180–181, 181–199.

Dimitrijević, M.D., 1997. Geology of Yugoslavia. second ed. Geoinstitute, Belgrade, Belgrade.

Dimitrijevic, M.N., Dimitrijevic, M.D., 1987. The turbiditic basins of Serbia. Serbian Academy of Sciences and Arts Department of Natural & Mathematical Sciences (380 pp.).

Djeric, N., Gerzina, N., Schmid, S.M., 2007. Age of the Jurassic Radiolarian Chert Formation from the Zlatar Mountain (SW Serbia). Ofioliti 32, 101–108.

Doglioni, C., Carminati, E., Cuffaro, M., Scrocca, D., 2007. Subduction kinematics and dynamic constraints. Earth-Sci. Rev. 83, 125–175.

Donelick, R.A., 1993. Apatite etching characteristics versus chemical composition. Nucl. Tracks Radiat. Meas. 21, 604.

Dunkl, I., 2002. Trackkey: a Windows program for calculation and graphical presentation of fission track data. Comput. Geosci.-Uk 28, 3–12.

Faccenna, C., Piromallo, C., Crespo-Blanc, A., Jolivet, L., Rosetti, F., 2004. Lateral slab deformation and the origin of the western Mediterranean arcs. Tectonics 23, TC1012 (doi: 1010.1029/2002TC001488).

Froitzheim, N., Conti, P., van Daalen, M., 1997. Late Cretaceous, synorogenic, low-angle normal faulting along the Schlinig fault (Switzerland, Italy, Austria) and its significance for the tectonics of the Eastern Alps. Tectonophysics 280, 267–293.

Fodor, L., Csontos, L., Bada, G., Györfi, I., Benkovics, L., 1999. Tertiary tectonic evolution of the Pannonian basin system and neighbouring orogens: a new synthesis of paleostress data. In: Durand, B., Jolivet, L., Horvath, F., Seranne, M. (Eds.), The Mediteranean basins: Tertiary extension within the Alpine orogen. The Geological Society, London, pp. 295–334.

Foeken, J.P.T., 2004. Tectono-morphology of the Ligurian Alps and Adjacent Basins (NW Italy): An Integrated Study of Their Neogene to Present evolution. [Ph.D. thesis]. Vrije Universiteit, Amsterdam, The Netherlands (192 p.).

Fügenschuh, B., Schmid, S.M., 2005. Age and significance of core complex formation in a very curved orogen: evidence from fission track studies in the South Carpathians (Romania). Tectonophysics 404, 33–53.

Galbraith, R.F., Laslett, G.M., 1993. Statistical-models for mixed fission-track ages. Nucl. Tracks Radiat. Meas. 21, 459–470.

Gallhofer, D., von Quadt, A., Peytcheva, I., Schmid, S.M., Heinrich, C.A., 2015. Tectonic, magmatic, and metallogenic evolution of the Late Cretaceous arc in the Carpathian-Balkan orogen. Tectonics 34:1813–1836. http://dx.doi.org/10.1002/2015TC00383.

Garver, J.I., 2003. Etching zircon age standards for fission-track analysis. Radiat. Meas. 37, 47–53.

Gehrels, G.E., Valencia, V., Ruiz, J., 2008. Enhanced precision, accuracy, efficiency, and spatial resolution of U-Pb ages by laser ablation–multicollector–inductively coupled plasma–mass spectrometry. Geochem. Geophys. Geosyst. 9, Q03017. http://dx.doi.org/10.1029/2007GC001805.

Gleadow, A.J.W., Duddy, I.R., 1981. A natural long-term track annealing experiment for apatite. Nucl. Tracks 5, 169–174.

Goričan, Š., Košir, A., Rožič, B., Šmuc, A., Gale, L., Kukoč, D., Celarc, B., Črne, A.E., Kolar-Jurkovšek, T., Placer, L., 2012. Mesozoic deep-water basins of the eastern Southern Alps (NW Slovenia). J. Alp. Geology 55, 1–44.

Green, P.F., 1985. Comparison of Zeta calibration baselines for fission-track dating of apatite, zircon and sphene. Chem. Geol. 58, 1–22.

Grubić, A., 1999. Tectonics of Jastrebac and its general meaning. Tehnika – Rudarstvo, geologija i metalurgija 50, 13–17.

Hall, R., Cottam, M.A., Wilson, M.E.J., 2011. The SE Asian gateway: history and tectonics of the Australia–Asia collision. Geol. Soc. Lond., Spec. Publ. 355, 1–6.

Horváth, F., Bada, G., Szafian, P., Tari, G., Adam, A., Cloetingh, S., 2006. Formation and deformation of the Pannonian Basin: constraints from observational data. Geol. Soc. Lond. Mem. 32, 191–206.

Horváth, F., Musitz, B., Balázs, A., Végh, A., Uhrin, A., Nádor, A., Koroknai, B., Pap, N., Tóth, T., Wórum, G., 2015. Evolution of the Pannonian basin and its geothermal resources. Geothermics 53, 328–352.

Iancu, V., Berza, T., Seghedi, A., Gheuca, I., Hann, H.-P., 2005. Alpine polyphase tectonometamorphic evolution of the South Carpathians: a new overview. Tectonophysics 410, 337–365.

Ismail-Zadeh, A., Matenco, L., Radulian, M., Cloetingh, S., Panza, G., 2012. Geodynamics and intermediate-depth seismicity in Vrancea (the south-eastern Carpathians): current state-of-the art. Tectonophysics 530-531, 50–79.

Jolivet, L., Faccenna, C., 2000. Mediterranean extension and the Africa-Eurasia collision. Tectonics 19, 1095–1106.

Karamata, S., 2006. The geological development of the Balkan Peninsula related to the approach, collision and compression of Gondwanan and Eurasian units. In: Robertson, A.H.F., Mountrakis, D. (Eds.), Tectonic Development of the Eastern Mediterranean Region. Geological Society. Special Publications, London, pp. 155–178.

Karamata, S., Stefanović, D., Krstić, B., 2003. Permian to Neogene accretion of the assemblage of geologic units presently occuring to the south of the Pannonian Basin - Development of the Vardar Composite Terrane and adjacent units. Acta Geol. Hung. 46 (1), 63–76.

Ketcham, R.A., Donelick, R.A., Carlson, W.D., 1999. Variability of apatite fission-track annealing kinetics; III, extrapolation to geological time scales. Am. Mineral. 84, 1235–1255.

Ketcham, R.A., Donelick, R.A., Donelick, M.B., 2003. AFTSolve: a program for multi-kinetic modeling of apatite fission-track data. Am. Mineral. 88, 929.

Kounov, A., Seward, D., Burg, J.-P., Bernoulli, D., Ivanov, Z., Handler, R., 2010. Geochronological and structural constraints on the Cretaceous thermotectonic evolution of the Kraishte zone, western Bulgaria. Tectonics 29, TC2002. http://dx.doi.org/10.1029/2009tc002509.

Krautner, H.G., Krstic, B., 2002. Alpine and Pre-Alpine Units Within the South Carpathians and the Eastern Balkanides. Proceedings XVII CBGA Congress, Bratislava, pp. 245–257.

Krstić, B., Veselinović, M., Divljan, M., Rakić, M., 1980. Explanatory Booklet of the Basic Geological Map of the SFR Yugoslavia, Sheet Aleksinac 1:100000, Savezni geološki zavod, Beograd (in Serbian, English and Russian Summaries) (55 pp.).

Kydonakis, K., Gallagher, K., Brun, J.-P., Jolivet, M., Gueydan, F., Kostopoulos, D., 2014. Upper Cretaceous exhumation of the western Rhodope Metamorphic Province (Chalkidiki Peninsula, northern Greece). Tectonics 33, 1113–1132.

Laslett, G.M., Green, P.F., Duddy, I.R., Gleadow, A.J.W., 1987. Thermal annealing of fission tracks in apatite 2: a quantitative analysis. Chem. Geol. 65, 1–13.

Ludwig, K.R., 2005. User's Manual for Isoplot/Ex, Version 3.11. A Geochronological Toolkit for Microsoft Excel. Geochronology Center Special Publication, Berkeley.

Luijendijk, E., Van Balen, R.T., Ter Voorde, M., Andriessen, P.A.M., 2011. Reconstructing the Late Cretaceous inversion of the Roer Valley Graben (southern Netherlands) using a new model that integrates burial and provenance history with fission track thermochronology. J. Geophys. Res. Solid Earth 116:B6. http://dx.doi.org/10.1029/2010JB008071.

Malešević, M., Vukanović, M., Brković, T., Karajičić, L., Obradinović, Z., Stanisavljević, R., Dimitrijević, M., Urošević, M., 1980. Explanatory Booklet of the Basic Geological Map of the SFR Yugoslavia, Sheet Kuršumlija 1:100000, Savezni geološki zavod, Beograd (in Serbian, English and Russian summaries) (58 pp.).

Marović, M., Djoković, I., Toljić, M., Spahić, D., Milivojević, J., 2007. Extensional unroofing of the Veliki Jastrebac Dome (Serbia). Annales Geologiques de la Peninsule Balkanique 68, 21–27.

Matenco, L., Munteanu, I., ter Borgh, M., Stanica, A., Tilita, M., Lericolais, G., Dinu, C., Oaie, G., 2016. The interplay between tectonics, sediment dynamics and gateways evolution in the Danube system from the Pannonian Basin to the western Black Sea. Sci. Total Environ. 543, 807–827.

Matenco, L., Radivojević, D., 2012. On the formation and evolution of the Pannonian Basin: Constraints derived from the structure of the junction area between the Carpathians and Dinarides. Tectonics 31, TC6007. http://dx.doi.org/10.1029/2012tc003206.

Meinhold, G., Kostopoulos, D., Frei, D., Himmerkus, F., Reischmann, T., 2010. U–Pb LA-SF-ICP-MS zircon geochronology of the Serbo-Macedonian Massif, Greece: palaeotectonic constraints for Gondwana-derived terranes in the Eastern Mediterranean. Int. J. Earth Sci. 99, 813–832.

Missoni, S., Gawlick, H.-J., Sudar, M., Jovanović, D., Lein, R., 2012. Onset and demise of the Wetterstein Carbonate Platform in the mélange areas of the Zlatibor Mountain (Sirogojno, SW Serbia). Facies 58, 95–111.

Mladenović, A., Trivić, B., Cvetković, V., 2015. How tectonics controlled post-collisional magmatism within the Dinarides: inferences based on study of tectono-magmatic events in the Kopaonik Mts. (Southern Serbia). Tectonophysics 646, 36–49.

Monjoie, P., Lapierre, H., Tashko, A., Mascle, G.H., Dechamp, A., Muceku, B., Brunet, P., 2008. Nature and origin of the Triassic volcanism in Albania and Othrys: a key to understanding the Neotethys opening? Bull. Soc. Geol. Fr. 179, 411–425.

Morley, C.K., 2012. Late Cretaceous - Early Palaeogene tectonic development of SE Asia. Earth Sci. Rev. 115, 37–75.

Neubauer, F., Bojar, A.-V., 2013. Origin of sediments during Cretaceous continent-continent collision in the Romanian South Carpathians: preliminary constraints from 40Ar/39Ar single-grain dating of detrital white mica. Geol. Carpath. 56, 375–382 (b-b).

Pamić, J., 2002. The Sava-vardar Zone of the Dinarides and Hellenides versus the Vardar Ocean. Eclogae Geol. Helv. 95, 99–113.

Pamic, J.J., 1984. Triassic magmatism of the Dinarides in Yugoslavia. Tectonophysics 109, 273–307.

Pantić, V., Rakić, M., Hadži-Vuković, M., 1969. Paleogene sediments and younger granodiorites on the northern slope of Veliki Jastrebac. Zapisnici Srpskog geološkog društva za 1966. godinu 633–635 (in Serbian).

Pubellier, M., Meresse, F., 2013. Phanerozoic growth of Asia: geodynamic processes and evolution. J. Asian Earth Sci. 72, 118–128.

Rakić, M., Hadži-Vuković, M., Dimitrijević, M., Kalenić, M., Marković, V., 1976. Explanatory Booklet of the Basic Geological Map of the SFR Yugoslavia, Sheet Kruševac 1:100000, Savezni geološki zavod, Beograd (in Serbian, English and Russian Summaries) (63 pp.).

Rakić, M., Simonović, S., Hadži-Vuković, M., 1972. One more contribution to the geology and stratigraphy of the Veliki Jastrebac. Zapisnici Srpskog geološkog društva za 1969. godinu 3–6 (in Serbian).
Ramovš, A., Hinterlechner-Ravnik, A., Kalenić, M., Karamata, S., Kochansky-Devidé, V., Mirković, M., Petkovski, P., Sremac, J., Krstić, B., Kulenović, E., Temkova, V., 1989. Stratigraphic correlation forms of Yugoslav Paleozoic. Rendiconti. Società Geologica Italiana 12, 359–383.
Robertson, A., Karamata, S., Saric, K., 2009. Overview of ophiolites and related units in the Late Paleozoic-Early Cenozoic magmatic and tectonic development of Tethys in the northern part of the Balkan region. Lithos 108, 1–36.
Robertson, A.H.F., 2006. Contrasting modes of ophiolite emplacement in the Eastern Mediterranean region. Geol. Soc. Lond. Mem. 32, 235–261.
Săndulescu, M., 1984. Geotectonica României (translated title: Geotectonics of Romania). Ed. Tehnică, Bucharest (450 pp.).
Săndulescu, M., 1988. Cenozoic tectonic history of the Carpathians. In: Royden, L.H., Horvath, F. (Eds.), The Pannonian Basin, a Study in Basin Evolution. AAPG Memoir Vol. 45, pp. 17–25.
Schefer, S., 2010. Tectono-metamorphic and Magmatic Evolution of the Internal Dinarides (Kopaonik area, southern Serbia) and its Significance for the Geodynamic Evolution of the Balkan Peninsula, Philosophisch-Naturwissenschaftlichen Fakultät der Universität Basel. Universitat Basel, Basel (230 pp.).
Schefer, S., Cvetković, V., Fügenschuh, B., Kounov, A., Ovtcharova, M., Schaltegger, U., Schmid, S., 2011. Cenozoic granitoids in the Dinarides of southern Serbia: age of intrusion, isotope geochemistry, exhumation history and significance for the geodynamic evolution of the Balkan Peninsula. Int. J. Earth Sci. 100, 1181–1206.
Schefer, S., Egli, D., Missoni, S., Bernoulli, D., Gawlick, H.-J., Jovanović, D., Krystyn, L., Lein, R., Schmid, S.M., Sudar, M., 2010. Triassic sediments in the Internal Dinarides (Kopaonik area, southern Serbia): stratigraphy, paleogeographic and tectonic significance. Geol. Carpath. 61, 89–109.
Schmid, S., Bernoulli, D., Fügenschuh, B., Matenco, L., Schefer, S., Schuster, R., Tischler, M., Ustaszewski, K., 2008. The Alpine-Carpathian-Dinaridic orogenic system: correlation and evolution of tectonic units. Swiss J. Geosci. 101, 139–183.
Stojadinović, U., Matenco, L., Andriessen, P.A.M., Toljić, M., Foeken, J.P.T., 2013. The balance between orogenic building and subsequent extension during the Tertiary evolution of the NE Dinarides: constraints from low-temperature thermochronology. Glob. Planet. Chang. 103, 19–38.
Stojadinović, U., Matenco, L., Andriessen, P., Toljić, M., 2016. Structure and provenance of Late Cretaceous - Miocene sediments located near the NE Dinarides margin: inferences from kinematics and detrital thermochronology. Tectonophysics (this issue).
Tagami, T., 2005. Zircon fission-track thermochronology and applications to fault studies. Low Temperature Thermochronology: Techniques, Interpretations, and Applications, Reviews in Mineralogy and Geochemistry. Vol. 58, pp. 95–122.
Tari, G., Dovenyi, P., Dunkl, I., Horvath, F., Lenkey, L., Ştefănescu, M., Szafian, P., Toth, T., 1999. Lithospheric structure of the Pannonian basin derived from seismic, gravity and geothermal data. In: Durand, B., Jolivet, L., Horvath, F., Serrane, M. (Eds.), The Mediterranean Basins: Extension Within the Alpine Orogen Vol. 156. Geological Society of London Special Publications, pp. 215–250.
Tari, G., Horváth, F., Rumpler, J., 1992. Styles of extension in the Pannonian basin. Tectonophysics 208, 203–219.
Toljić, M., 2006. Geological Settings of Central Vardar Zone Between Avala Mts. and Kosmaj Mts. (PhD thesis). University of Belgrade, Faculty of Mining and Geology, Belgrade, p. 162.
Toljić, M., Matenco, L., Ducea, M.N., Stojadinović, U., Milivojević, J., Đerić, N., 2013. The evolution of a key segment in the Europe–Adria collision: the Fruška Gora of northern Serbia. Glob. Planet. Chang. 103, 39–62.
Ustaszewski, K., Kounov, A., Schmid, S.M., Schaltegger, U., Krenn, E., Frank, W., Fügenschuh, B., 2010. Evolution of the Adria-Europe plate boundary in the northern Dinarides: from continent-continent collision to back-arc extension. Tectonics 29, TC6017 (doi: 6010.1029/2010tc002668).
Ustaszewski, K., Schmid, S.M., Lugovic, B., Schuster, R., Schaltegger, U., Bernoulli, D., Hottinger, L., Kounov, A., Fügenschuh, B., Schefer, S., 2009. Late Cretaceous intra-oceanic magmatism in the internal Dinarides (northern Bosnia and Herzegovina): implications for the collision of the Adriatic and European plates. Lithos 108, 106–125.
van Gelder, I.E., Matenco, L., Willingshofer, E., Tomljenović, B., Andriessen, P.A.M., Ducea, M.N., Beniest, A., Gruić, A., 2015. The tectonic evolution of a critical segment of the Dinarides-Alps connection: kinematic and geochronological inferences from the Medvednica Mountains, NE Croatia. Tectonics 34:1952–1978. http://dx.doi.org/10.1002/2015TC003937.
Vergés, J., Fernàndez, M., 2012. Tethys–Atlantic interaction along the Iberia–Africa plate boundary: the Betic–Rif orogenic system. Tectonophysics 579, 144–172.
von Quadt, A., Moritz, R., Peytcheva, I., Heinrich, C.A., 2005. Geochronology and geodynamics of Late Cretaceous magmatism and Cu-Au mineralization in the Panagyurishte region of the Apuseni-Banat-Timok-Srednogorie belt, Bulgaria. Ore Geol. Rev. 27, 95–126.
Wernicke, B., 1985. Uniform-sense normal simple shear of the continental lithosphere. Can. J. Earth Sci. 22, 108–125.
Wortel, M.J.R., Spakman, W., 2000. Subduction and slab detachment in the Mediteranean-Carpathian region. Science 290, 1910–1917.
Zweigel, P., Ratschbacher, L., Frisch, W., 1998. Kinematics of an arcuate fold-thrust belt: the southern Eastern Carpathians (Romania). Tectonophysics 297, 177–207.